รายงานวิจัยฉบับสมบูรณ์

โครงการ ควอนตัมดอทแบบสนามแม่เหล็กของสารกึ่งตัวนำที่ผสมไอออนสารแม่เหล็กอย่างเบาบาง

โดย

ด.ร. อรรถพล อ่ำทอง

มีนาคม 2558

สัญญาเลขที่ R2557C123

รายงานวิจัยฉบับสมบูรณ์

โครงการ ควอนตัมดอทแบบสนามแม่เหล็กของสารกึ่งตัวนำ ที่ผสมไอออนสารแม่เหล็กอย่างเบาบาง

คณะผู้วิจัย สังกัด

ดร.อรรถพล อ่ำทอง สังกัดภาควิชาฟิสิกส์ คณะวิทยาศาสตร์

สนับสนุนโดยกองทุนมหาวิทยาลัยนเรศวร

บทคัดย่อ

งานวิจัยนี้ศึกษาควอนตัมดอทวงกลมจากสารกึ่งตัวนำที่ผสมไอออนสารแม่เหล็กอย่างเบาบางในสนามแม่เหล็กสม่ำเสมอ พลังงานและสถานะของอิเล็กตรอนซึ่งขังในควอนตัมดอทคำนวณโดยใช้การประมาณของมวลเอฟเฟคทีฟ เราแสดงให้เห็นว่าพลังงานของอิเล็กตรอนสปินขึ้นและลงขึ้นอยู่กับค่าจีเอฟเฟคทีฟ และยังพบการกระจายตัวของอิเล็กตรอนซึ่งขึ้นอยู่กับสปิน นอกจากนี้ยังแนะนำการประมาณระดับพลังงานดังกล่าว

Executive Summary

โครงการนี้ได้เสนอแบบจำลองควอนตัมดอทของสารกึ่งตัวนำที่ผสมสารแม่เหล็กอย่างเบาบางและสารกึ่งตัวนำธรรมดาในสนานแม่เหล็กสม่ำเสมอ ในสถานการณ์ที่สารกึ่งตัวนำทั้งสองมีแถบพลังงานไม่ต่างกันมากเมื่อเทียบกับการแยกชั้นของพลังงานจากปรากฏการณ์ซีแมน ระดับพลังงานและฟังก์ชันคลื่นของอิเล็กตรอนในควอนตัมดอทนี้หาได้จากการเชื่อมฟังก์ชันคลื่นในบริเวณรอยต่อ เราพบว่าการแยกชั้นพลังงานของซีแมนสามารถนำมาช่วยในการควบคุมการกระจายตัวของอิเล็กตรอนสปินขึ้นและสปินลงได้ โดยอิเล็กตรอนสปินขึ้นจะถูกขังในภายในควอนตัมดอท ขณะที่อิเล็กตรอนสปินลงจะกระจายตัวอยู่ภายนอก แต่หากพลังงานของอิเล็กตรอนมีมาก ทั้งอิเล็กตรอนสปินขึ้นและลงจะกระจายตัวทั้งภายนอกและภายในควอนตัมดอท ผลจากการศึกษานี้อาจนำไปใช้ประโยชน์ในการประยุกต์ทางด้านสปินทรอนิกส์

สารบัญเรื่อง

1. บทนำ

A diluted magnetic semiconductor (DMS) [1–3] is a compound semiconductor formed by doping of a nonmagnetic semiconductor (NMS) by magnetic ions. Magnetic properties in a DMS caused by the impurities have attracted much attention. In a paramagnetic DMS, an external magnetic field gives rise to not only the normal Zeeman splitting but also the strong exchange interaction between band electrons in a DMS and those associated with magnetic ions. As a result, the energy splitting is extremely enhanced. This phenomenon can be interpreted by introducing the effective g-factor (g_{eff}) which is much larger than the g-factor of band electrons. Experimental studies show the value of g_{eff} can be tuned to several hundreds, depending upon magnetic concentration, temperature, and host semiconductors [4,5].

According to the giant Zeeman effect, a DMS has become one of the most potential materials for spintronic application which aims to manipulate spin and charge of carriers [6,7]. One example of the application is spin polarized bound states which are created in a DMS layer in the presence of nonhomogeneous magnetic fields associated with permalloy disks, Abrikosov vortices, and Josephson vortices [8–10]. When g_{eff} is sufficiently large, the Zeeman energy will become a major confinement potential, while the potential due to a magnetic vector potential can be neglected. The energy spectrum of the Zeeman-bound states is therefore found to be influenced by magnetic field profiles.

Another possibility is to use a DMS as a tunnel junction. It was first investigated by Egues [11] who focused on the ZnSe/ZnMnSe/ZnSe heterostructure. Based on the concept that spin up and spin down electrons feel different potentials in the region of a DMS, a spin-polarized current can be achieved after injected electrons tunnel through a DMS. Using the different method, Chang and Peeters [12] revisited the problem to support the work of Egues. They additionally investigated the effect of the DMS thickness on spin-dependent conductivity. In the other studies of the heterostructure [13–15], the effects of the Mn concentration, conduction band offset, and applied electric field are included to improve the spin polarization. The results from related systems consisting of DMSs also show the possibility of spin-polarized tunnelling [16–18].

Moreover, DMSs are applied to quantum dots. They have been studied for different geometries: a cylinder, a sphere, and a cuboid [19–24]. Interestingly, Triki et al. [25] proposed the quantum dot heterostructure which is formed by CdMnSe (CdSe) in the shape of a truncated cone surrounded by ZnSe (ZnMnSe) and numerically studied the variation of electron energies as a function of a magnetic field. In the heterostructure, the potential due to the band offset, which is discussed intensively, plays a major role in electron confinement while the giant Zeeman potential only leads to energy splitting of spin up and spin down states.

In this work, we analytically investigate the DMS/NMS quantum dot formed by a disk-shaped DMS surrounded by a NMS as depicted in Fig. 1, focusing on the effect of the giant Zeeman potential. To see the effect clearly, we study the quantum dot where a host semiconductor of a DMS is the same material as a surrounding NMS. In this heterostructure, only the confinement due to the giant Zeeman potential exists while the band offset at the interface can be ignored. The spin-dependent energy spectrum and distribution of electron states are discussed and classified. Without the band offset, we find spin up and spin down states exhibit completely different spatial distribution. These behaviors of spin states may be useful for the application of spin-based memories or future spintronic devices [26–28].

2. ทฤษฎี

Within the mean field approximation, the potential energy of a conduction band electron travelling in a DMS subjected to a magnetic field $\vec{B} = B\hat{z}$ is given by

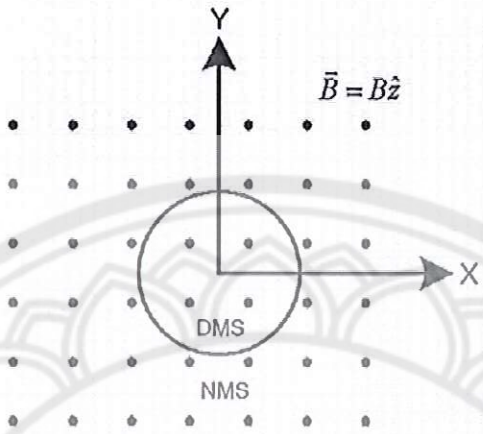

Fig. 1. The hybrid system of a circular DMS surrounded by a NMS in a uniform magnetic field $\vec{B} = B\hat{z}$ represented by the symbol •.

$$V = \frac{1}{2}g^*\mu_B\sigma_z B - \frac{1}{2}N_0\alpha x\langle S_z\rangle\sigma_z, \tag{1}$$

where the first term is the Zeeman splitting energy and the second one is the potential associated with the exchange interaction between electrons in the conduction band and those of doped magnetic ions. In this equation, g^* is the electron g-factor, σ_z is the z component of Pauli matrices, $N_0\alpha$ is the exchange constant, x is magnetic concentration, and $\langle S_z\rangle$ is the average spin per magnetic site. Because $\langle S_z\rangle$ only exists when a magnetic field is non-vanishing. It is more convenient to write the potential as

$$V = -\frac{1}{2}g_{\text{eff}}\mu_B\sigma_z B, \tag{2}$$

where $g_{\text{eff}} = -g^* + \frac{N_0\alpha x\langle S_z\rangle}{\mu_B B}$ is the effective g-factor [8].

In our study, the layer of DMS/NMS heterostructure placed on x–y plane in the presence of a magnetic field $\vec{B} = B\hat{z}$ is investigated. For simplicity, we assume that electrons move effectively in the plane. Within the effective mass approximation, the Hamiltonian in cylindrical coordinates (r, ϕ, z) describing a single electron $(q = -e)$ in the layer is

$$\hat{H} = \frac{(\hat{p} + e\vec{A})^2}{2M} - \frac{1}{2}g_{\text{eff}}\mu_B\sigma_z B\Theta(R - r), \tag{3}$$

where M is the effective mass of an electron, R is the radius of a circular DMS, and Θ is the Heaviside step function. Here, the conventional Zeeman interaction outside the dot region $(r \geqslant R)$ is vanishingly small, compared to the giant Zeeman interaction existing inside. The symmetric gauge $\vec{A} = (Br/2)\hat{\phi}$ is chosen in our calculation. Due to the rotational symmetry of the Hamiltonian, the general form of the eigenfunction can be expressed as

$$\Psi^{\sigma}_{nm}(r, \phi) = e^{im\phi}\psi^{\sigma}_{nm}(r)\chi_{\sigma}, \tag{4}$$

where n, m, and σ refer to a radial quantum number, an angular momentum and spin ($\uparrow$ or $\downarrow$) respectively. $\chi_{\uparrow\downarrow}$ is the column matrix representing a spin up $\begin{pmatrix}1\\0\end{pmatrix}$ or spin down $\begin{pmatrix}0\\1\end{pmatrix}$ state. After substituting the wavefunction (4) into the Schrödinger equation and using the relation $\sigma_z\chi_\sigma = \sigma\chi_\sigma$ where σ is 1 and -1 for spin up and spin down respectively, we obtain the radial equation

$$-\frac{\hbar^2}{2M}\left(\frac{\partial^2}{\partial r^2}+\frac{1}{r}\frac{\partial}{\partial r}-\frac{m^2}{r^2}\right)\psi^{\sigma}_{nm}(r)+\left(\frac{m\hbar\omega_c}{2}+\frac{M\omega_c^2 r^2}{8}\right)\psi^{\sigma}_{nm}(r)-\left(\frac{\sigma g_{\text{eff}}\mu_B B\Theta(R-r)}{2}\right)\psi^{\sigma}_{nm}(r)$$
$$=E\psi^{\sigma}_{nm}(r), \tag{5}$$

where $\omega_c = eB/M$ is the cyclotron frequency. We then measure all of the quantities in the following units: $r=\rho\ell$, $E=\epsilon\hbar\omega_c$, and $M=m^*M_e$ where $\ell=\sqrt{\hbar/eB}$ is the magnetic length and M_e is the electron rest mass. The Schrödinger equation is rewritten in the dimensionless form

$$\left(-\frac{1}{2}\frac{\partial^2}{\partial\rho^2}-\frac{1}{2\rho}\frac{\partial}{\partial\rho}+\frac{m^2}{2\rho^2}+\frac{m}{2}+\frac{\rho^2}{8}-\frac{\sigma g_{\text{eff}}m^*\Theta(R/\ell-\rho)}{4}\right)\psi^{\sigma}_{nm}(\rho)=\epsilon\psi^{\sigma}_{nm}(\rho). \tag{6}$$

After that, we define another variable $x=\rho^2/2$. The Schrödinger equation now becomes

$$\left(x\frac{\partial^2}{\partial x^2}+\frac{\partial}{\partial x}-\frac{x}{4}-\frac{m^2}{4x}+\beta(x)\right)\psi^{\sigma}_{nm}(x)=0, \tag{7}$$

where

$$\beta(x)=\begin{cases}\beta_\sigma & x<R^2/(2\ell^2)\\ \beta_0 & x\geqslant R^2/(2\ell^2),\end{cases} \tag{8}$$

$\beta_\sigma=\beta_0+(\sigma g_{\text{eff}}m^*/4)$, and $\beta_0=\epsilon-m/2$. Considering the solutions when x is close to 0 and infinity, we find the wavefunction $\psi^{\sigma}_{nm}(x)$ can be expressed as $\psi^{\sigma}_{nm}(x\to 0)=x^{|m|/2}$ and $\psi^{\sigma}_{nm}(x\to\infty)=e^{-x/2}$. Therefore, the general solution of Eq. (7) is given by

$$\psi^{\sigma}_{nm}(x)=x^{|m|/2}e^{-x/2}w(x). \tag{9}$$

To find the solution inside the quantum dot ($r<R$) where $\beta(x)=\beta_\sigma$, we substitute the wavefunction (9) into the Schrödinger Eq. (7) and yield the Kummer's equation [29]

$$x\frac{\partial^2 w}{\partial x^2}+(|m|+1-x)\frac{\partial w}{\partial x}-\left(\frac{|m|}{2}+\frac{1}{2}-\beta_\sigma\right)w=0, \tag{10}$$

whose solution is

$$w(x)=C_1M\left(\frac{|m|}{2}+\frac{1}{2}-\beta_\sigma,|m|+1,x\right)+C_2U\left(\frac{|m|}{2}+\frac{1}{2}-\beta_\sigma,|m|+1,x\right), \tag{11}$$

where C_1 and C_2 are arbitrary constants. M and U are a Kummer-M function and Kummer-U function respectively. Because $x^{|m|/2}e^{-x/2}U\left(\frac{|m|}{2}+\frac{1}{2}-\beta_\sigma,|m|+1,x\right)$ diverges when x approaches 0, we choose $C_2=0$ to obtain a Kummer-M function as the solution inside the quantum dot.

Outside the quantum dot region ($r\geqslant R$) where the giant Zeeman interaction vanishes, we can find the solution in the same way we did before. In this case, we also get the solution in the form of a Kummer-M function and Kummer-U function as shown in Eq. (11), but β_σ is replaced by β_0. When x approaches infinity, a Kummer-M function $M\left(\frac{|m|}{2}+\frac{1}{2}-\beta_0,|m|+1,x\right)$ is proportional to $e^x x^{\left(-\frac{|m|}{2}-\frac{1}{2}-\beta_0\right)}$. This causes the wavefunction $\psi^{\sigma}_{nm}(x)$ to diverge. Hence, we choose $C_1=0$ in this case to get a Kummer-U function as the solution outside the quantum dot. The radial wavefunction corresponding to the Schrödinger Eq. (6) is expressed in term of ρ as

$$\psi^{\sigma}_{nm}(\rho)=\begin{cases}C_1e^{-\rho^2/4}\rho^{|m|}M(-a_1,b,\rho^2/2) & \rho<\sqrt{2s}\\ C_2e^{-\rho^2/4}\rho^{|m|}U(-a_2,b,\rho^2/2) & \rho\geqslant\sqrt{2s},\end{cases} \tag{12}$$

where $a_1=\beta_\sigma-|m|/2-1/2$, $a_2=\beta_0-|m|/2-1/2=a_1-\sigma g_{\text{eff}}m^*/4$, and $b=|m|+1$. s is the dimensionless parameter defined by $s=B\pi R^2/(h/e)=\Phi/\Phi_0;\Phi=B\pi R^2$ and $\Phi_0=h/e$. It determines the magnetic flux Φ passing through the quantum dot region in the unit of the flux quantum Φ_0. At the edge of the dot where $r=R$, we have the corresponding $\rho=\sqrt{2s}$. Now, C_1 and C_2 are constants satisfying the normalization condition $\int_0^{2\pi}\int_0^{\infty}\Psi^*\Psi r dr d\phi=1$. From the definition of a_1, the eigenenergy can be expressed as

$$\epsilon_{nm}^{\sigma} = a_1 + \frac{m}{2} + \frac{|m|}{2} + \frac{1}{2} - \frac{\sigma g_{\text{eff}} m^*}{4}. \tag{13}$$

To find the values of a_1, we match the radial wavefunctions inside and outside the quantum dot by the boundary condition, i.e., the logarithmic derivatives of the wavefunctions at the dot radius ($\rho = \sqrt{2s}$)

$$\frac{\mathrm{d}}{\mathrm{d}\rho} \ln \psi^{in}(\rho)\Big|_{\rho=\sqrt{2s}} = \frac{\mathrm{d}}{\mathrm{d}\rho} \ln \psi^{out}(\rho)\Big|_{\rho=\sqrt{2s}}. \tag{14}$$

This equation leads to

$$a_1 - a_1 \frac{M(1-a_1,b,s)}{M(-a_1,b,s)} = a_2 + a_2(a_2+b-1)\frac{U(1-a_2,b,s)}{U(-a_2,b,s)}, \tag{15}$$

which can be solved numerically to obtain the quantized values of a_1.

When g_{eff} is extremely large, it is obvious that the giant Zeeman potential $-\sigma g_{\text{eff}} m^*/4$ in Eq. (6) will greatly lower the energy levels of spin up states $\psi_{nm}^{\uparrow}(\rho)$. Then, the states are strongly confined in a very deep quantum well which is formed by the Zeeman potential existing inside the dot region. In this circumstance, we could assume that the spin up wavefunctions only distribute inside the dot region and vanish at the dot radius. With this approximation, the wavefunctions in Eq. (12) for spin up states become

$$\psi_{nm}^{\uparrow}(\rho) = Ae^{-\rho^2/4}\rho^{|m|}M(-a_1,b,\rho^2/2), \tag{16}$$

where $\psi_{nm}^{\uparrow}(\rho = \sqrt{2s}) = 0$. This boundary condition leads to

$$M\left(-\beta_\sigma + \frac{|m|}{2} + \frac{1}{2}, |m|+1, s\right) = 0. \tag{17}$$

Defining α_n^M as the n^{th} zero of the Kummer-M function, which satisfies $M(\alpha_n^M, |m|+1, s) = 0$, we obtain the approximated eigenenergies ($\epsilon_{\alpha pp}^{\uparrow}$) corresponding to the spin up states

$$\epsilon_{\alpha pp}^{\uparrow} = -\alpha_n^M + \frac{m}{2} + \frac{|m|}{2} + \frac{1}{2} - \frac{g_{\text{eff}} m^*}{4}. \tag{18}$$

Conversely, the giant Zeeman potential $-\sigma g_{\text{eff}} m^*/4$ will act as a very high barrier for spin down states, which does not allow the states to enter the dot region. In this case, we could assume that the spin down wavefunctions only distribute outside the dot region and vanish at the dot radius to get

$$\psi_{nm}^{\downarrow}(\rho) = Be^{-\rho^2/4}\rho^{|m|}U(-a_2,b,\rho^2/2), \tag{19}$$

where $\psi_{nm}^{\downarrow}(\rho = \sqrt{2s}) = 0$. This boundary condition leads to

$$U\left(-\beta_0 + \frac{|m|}{2} + \frac{1}{2}, |m|+1, s\right) = 0. \tag{20}$$

Defining α_n^U as the n^{th} zero of the Kummer-U function, which satisfies $U(\alpha_n^U, |m|+1, s) = 0$, we obtain the approximated eigenenergies ($\epsilon_{\alpha pp}^{\downarrow}$) corresponding to the spin down states

$$\epsilon_{\alpha pp}^{\downarrow} = -\alpha_n^U + \frac{m}{2} + \frac{|m|}{2} + \frac{1}{2}. \tag{21}$$

3. ผลการทดลอง

After solving Eq. (15) numerically, we obtain the quantized values of a_1 for spin up and spin down states, leading to the spin-dependent eigenenergies in Eq. (13) as shown in Fig. 2. In this calculation, $m^* = 0.5$ and $s = 4$, corresponding to a quantum dot radius $R = 100$ nm and a magnetic field of 0.5 T. To see the effect of the giant Zeeman potential clearly, the value of g_{eff} is varied in each panel of the figure. Note that g_{eff} can be controlled by temperature, magnetic concentration, and host semiconductors in experiments.

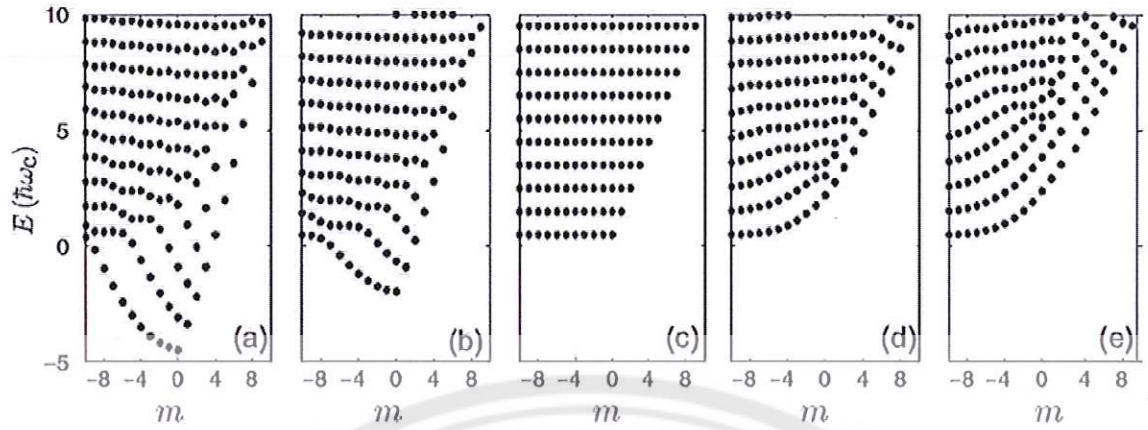

Fig. 2. The energy spectrum of spin up and spin down eigenstates for various values of g_{eff}. (a) $E^{\downarrow}$ with $g_{\text{eff}} = 40$, (b) $E^{\downarrow}$ with $g_{\text{eff}} = 20$, (c) $E^{\downarrow}$ and $E^{\uparrow}$ with $g_{\text{eff}} = 0$, (d) $E^{\uparrow}$ with $g_{\text{eff}} = 20$, and (e) $E^{\uparrow}$ with $g_{\text{eff}} = 40$.

Without the Zeeman potential ($g_{\text{eff}} = 0$), spin up and spin down states have the same energies as seen in Fig. 2(c). Because electrons only feel a uniform magnetic field, their energy levels are exactly the same as the well-known Landau levels [30]: $\epsilon = n + m/2 + |m|/2 + 1/2$. When g_{eff} is greater than zero, electrons additionally feel the discontinuous Zeeman potential. This leads to the energy spectrum which can be considered as Landau levels disturbed by the exchange interaction in a DMS region.

In Fig. 2(a) and (b), we see that some low-lying energy levels of spin up states tend to separate from the others with increasing of g_{eff}, resulting in two energy patterns concerning the distribution of wavefunctions. Examples of low-lying states represented by solid lines are shown in Fig. 3. Their energies are negative because the negative Zeeman potential $-g_{\text{eff}}m^*/4$ in Eq. (6) behaves like a quantum well to trap the states. For this reason, they are mostly localized inside the dot region and start decaying when extending outside. The high-energy excited states represented by dashed lines behave differently. Due to their positive energies, they are not confined by the Zeeman quantum well. As seen in Fig. 3, the states oscillate over the region both inside and outside the dot.

In the case of the spin down spectrum shown in Fig. 2(d) and (e), the Zeeman potential $g_{\text{eff}}m^*/4$ existing in the DMS region will act as a barrier to perturb Landau levels by raising the energy levels. We find low-lying states are pushed by the Zeeman barrier to the region outside. As seen in Fig. 4, the states with $n = 0$, 1, and 2 oscillate outside and decay when extending inside the dot region. If energies of excited states are greater than the Zeeman potential $g_{\text{eff}}m^*/4$, they will be able to extend over the region both inside and outside the dot. As seen in the figure, the states $\psi^{\downarrow}_{n=3,4,5}$ with energies 5.606, 6.095, and 7.099 can oscillate in the DMS region, where the Zeeman potential in the figure is $g_{\text{eff}}m^*/4 = 5$. Note that all energies are in the unit of $\hbar\omega_c$. Raising the value of g_{eff} will increase the number of the states which decay inside the dot region.

When $|m|$ is sufficiently large, both spin up and spin down states will behave like Landau states. Considering Eq. (6), one can see that the term $m^2/2\rho^2$ acts as a barrier which does not allow wavefunctions to enter the center of the quantum dot. As a result, the wavefunctions with large $|m|$ will extend far from the origin. In a classical viewpoint, electrons corresponding to the states with large $|m|$ will travel outside the dot region where the magnetic field is uniform and the Zeeman potential is zero. They do not feel the discontinuous Zeeman potential. Consequently, their eigenenergies and eigenstates are similar to Landau levels and Landau states respectively.

Fig. 5 shows the approximated eigenenergies of spin up and spin down states in the circumstance where the giant Zeeman potential is extremely large ($g_{\text{eff}} = 500$). We find that our spin up approximation agrees well with the eigenenergies of low-lying states with small $|m|$. This is because the spatial distribution of high energy states and the states with large $|m|$ is not consistent with the assumption in our approximation; they can penetrate deep into the region outside. On the other hand, the approximated eigenenergies of spin down states are found to be in good agreement when $|m|$ is sufficiently large. For each value of m, we see that the energies of excited states tend to differ from approximated values. This is because these states can penetrate deep into the dot region.

Without the Zeeman potential ($g_{\text{eff}} = 0$), spin up and spin down states have the same energies as seen in Fig. 2(c). Because electrons only feel a uniform magnetic field, their energy levels are exactly the same as the well-known Landau levels [30]: $\epsilon = n + m/2 + |m|/2 + 1/2$. When g_{eff} is greater than zero, electrons additionally feel the discontinuous Zeeman potential. This leads to the energy spectrum which can be considered as Landau levels disturbed by the exchange interaction in a DMS region.

In Fig. 2(a) and (b), we see that some low-lying energy levels of spin up states tend to separate from the others with increasing of g_{eff}, resulting in two energy patterns concerning the distribution of wavefunctions. Examples of low-lying states represented by solid lines are shown in Fig. 3. Their energies are negative because the negative Zeeman potential $-g_{\text{eff}}m^*/4$ in Eq. (6) behaves like a quantum well to trap the states. For this reason, they are mostly localized inside the dot region and start decaying when extending outside. The high-energy excited states represented by dashed lines behave differently. Due to their positive energies, they are not confined by the Zeeman quantum well. As seen in Fig. 3, the states oscillate over the region both inside and outside the dot.

In the case of the spin down spectrum shown in Fig. 2(d) and (e), the Zeeman potential $g_{\text{eff}}m^*/4$ existing in the DMS region will act as a barrier to perturb Landau levels by raising the energy levels. We find low-lying states are pushed by the Zeeman barrier to the region outside. As seen in Fig. 4, the states with $n = 0$, 1, and 2 oscillate outside and decay when extending inside the dot region. If energies of excited states are greater than the Zeeman potential $g_{\text{eff}}m^*/4$, they will be able to extend over the region both inside and outside the dot. As seen in the figure, the states $\psi^{\downarrow}_{n=3,4,5}$ with energies 5.606, 6.095, and 7.099 can oscillate in the DMS region, where the Zeeman potential in the figure is $g_{\text{eff}}m^*/4 = 5$. Note that all energies are in the unit of $\hbar\omega_c$. Raising the value of g_{eff} will increase the number of the states which decay inside the dot region.

When $|m|$ is sufficiently large, both spin up and spin down states will behave like Landau states. Considering Eq. (6), one can see that the term $m^2/2\rho^2$ acts as a barrier which does not allow wavefunctions to enter the center of the quantum dot. As a result, the wavefunctions with large $|m|$ will extend far from the origin. In a classical viewpoint, electrons corresponding to the states with large $|m|$ will travel outside the dot region where the magnetic field is uniform and the Zeeman potential is zero. They do not feel the discontinuous Zeeman potential. Consequently, their eigenenergies and eigenstates are similar to Landau levels and Landau states respectively.

Fig. 5 shows the approximated eigenenergies of spin up and spin down states in the circumstance where the giant Zeeman potential is extremely large ($g_{\text{eff}} = 500$). We find that our spin up approximation agrees well with the eigenenergies of low-lying states with small $|m|$. This is because the spatial distribution of high energy states and the states with large $|m|$ is not consistent with the assumption in our approximation; they can penetrate deep into the region outside. On the other hand, the approximated eigenenergies of spin down states are found to be in good agreement when $|m|$ is sufficiently large. For each value of m, we see that the energies of excited states tend to differ from approximated values. This is because these states can penetrate deep into the dot region.

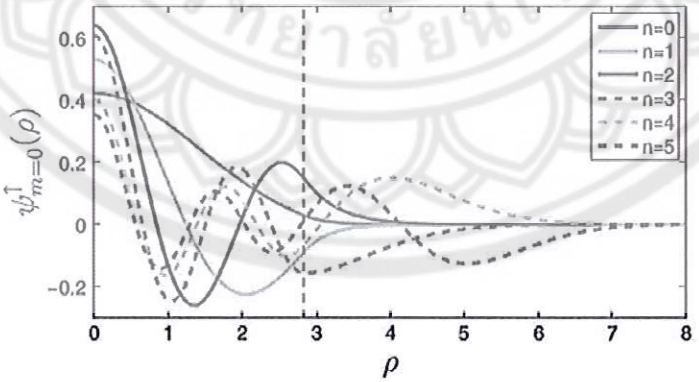

Fig. 3. Spin up radial wavefunctions with $m = 0$ corresponding to the eigenenergies in Fig. 2(a) where $g_{\text{eff}} = 40$. The black dashed line represents the dot radius where $\rho = \sqrt{8}$.

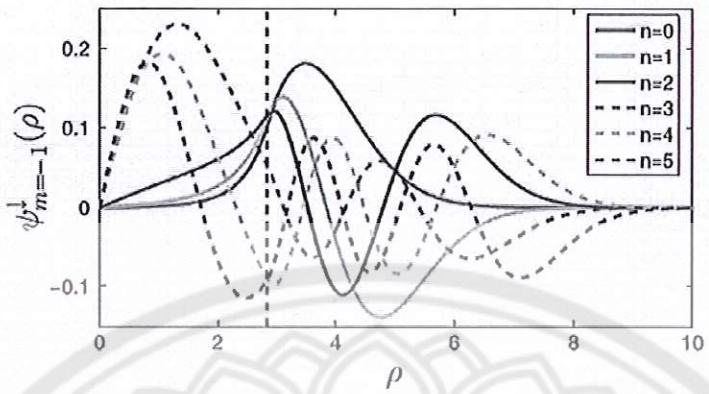

Fig. 4. Spin down radial wavefunctions with $m = -1$ corresponding to the eigenenergies in Fig. 2(e) where $g_{\text{eff}} = 40$. The black dashed line represents the dot radius where $\rho = \sqrt{8}$.

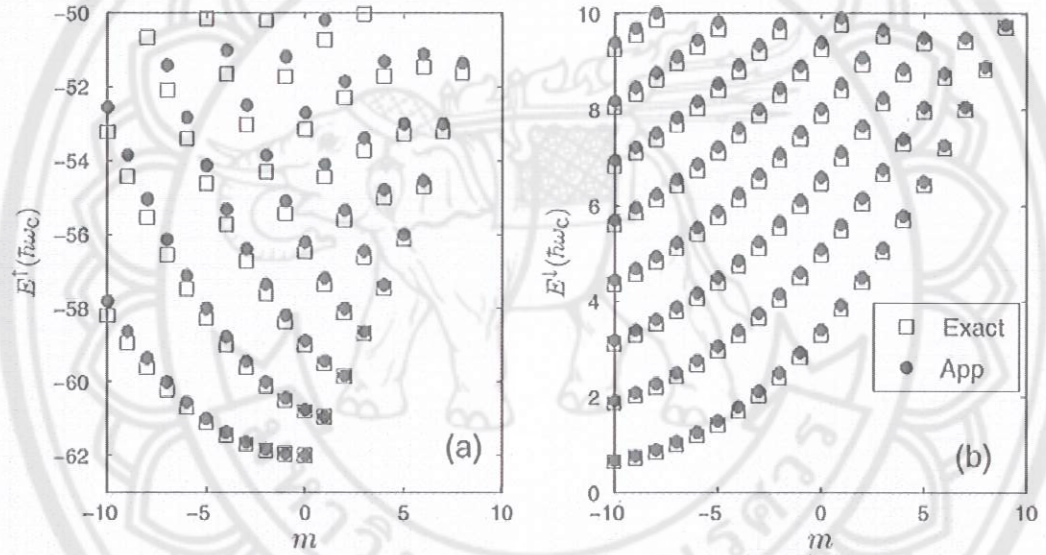

Fig. 5. Comparison of exact eigenenergies (squares) and approximated energies (points) when g_{eff} is 500, $s = 6$, and $m^* = 0.5$ for **(a)** spin up and (b) spin down.

4. สรุปผลการทดลอง

In conclusion, we have presented the quantum dot heterostructure of a DMS and a NMS in the presence of a uniform magnetic field, where a band offset at a mismatched interface is vanishingly small, compared to the giant Zeeman splitting. Spin-dependent eigenenergies and eigenstates describing electrons trapped in the quantum dot are derived by matching wavefunctions at the boundary. It is found that the Zeeman potential due to the exchange interaction in a DMS can be used to control the spin distribution of low-lying states. That is, spin up states are confined inside the dot region, while spin down states extend outside. If energies of spin states are sufficiently large, they will be able to distribute over the region both inside and outside the dot. These results may be useful for manipulating spin states in spintronic application. However, for the heterostructure where a band offset is significant the spin-dependent localization will not be found. We also calculate the approximated eigenenergies when g_{eff} is very large. Good approximation is found when spin up wavefunctions are strongly localized inside the dot area and spin down wavefunctions overwhelmingly distribute outside.

5. เอกสารอ้างอิง

[1] J.K. Furdyna, Diluted magnetic semiconductors: an interface of semiconductor physics and magnetism (invited), J. Appl. Phys. 53 (1982) 7637–7643.

[2] J.K. Furdyna, Diluted magnetic semiconductors, J. Appl. Phys. 64 (1988) R29–R64.

[3] W. de Jonge, H. Swagten, Magnetic properties of diluted magnetic semiconductors, J. Magn. Magn. Mater. 100 (1991) 322–345.

[4] A. Hundt, J. Puls, F. Henneberger, Spin properties of self-organized diluted magnetic $Cd_{1-x}Mn_x$ Se quantum dots, Phys. Rev. B 69 (2004) 121309.

[5] T. Dietl, M. Sawicki, M. Dahl, D. Heiman, E.D. Isaacs, M.J. Graf, S.I. Gubarev, D.L. Alov, Spin-flip scattering near the metal-to-insulator transition in $Cd_{0.95}Mn_{0.05}$ Se:In, Phys. Rev. B 43 (1991) 3154–3163.

[6] P. Kacman, Spin interactions in diluted magnetic semiconductors and magnetic semiconductor structures, Semicond. Sci. Technol. 16 (2001) R25.

[7] I. uti, J. Fabian, S. Das Sarma, Spintronics: fundamentals and applications, Rev. Mod. Phys. 76 (2004) 323–410.

[8] T.G. Rappoport, M. Berciu, B. Jankó, Effect of the Abrikosov vortex phase on spin and charge states in magnetic semiconductor–superconductor hybrids, Phys. Rev. B 74 (2006) 094502.

[9] M. Berciu, B. Jankó, Nanoscale Zeeman localization of charge carriers in diluted magnetic semiconductor–permalloy hybrids, Phys. Rev. Lett. 90 (2003) 246804.

[10] X.L. Wang, C.T. Lin, B. Liang, S. Yu, S. Ooi, K. Hirata, S.Y. Ding, D.Q. Shi, S.X. Dou, Z.W. Lin, J.G. Zhu, Josephson-vortex flow resistance in $Bi_2Sr_2Ca_2Cu_3O_y$ single crystals and its possible application in the manipulation of spin and charge textures in diluted magnetic semiconductors, J. Appl. Phys. 101 (2007) 09G116.

[11] J.C. Egues, Spin-dependent perpendicular magnetotransport through a tunable $ZnSe/Zn_{1-x}Mn_xSe$ heterostructure: a possible spin filter?, Phys Rev. Lett. 80 (1998) 4578–4581.

[12] K. Chang, F. Peeters, Spin polarized tunneling through diluted magnetic semiconductor barriers, Solid State Commun. 120 (2001) 181–184.

[13] Y. Guo, H. Wang, B.-L. Gu, Y. Kawazoe, Spin-polarized transport through a $ZnSe/Zn_{1-x}Mn_xSe$ heterostructure under an applied electric field, J. Appl. Phys. 88 (2000) 6614–6617.

[14] F. Zhai, Y. Guo, B.-L. Gu, Effects of conduction band offset on spin-polarized transport through a semimagnetic semiconductor heterostructure, J. Appl. Phys. 90 (2001) 1328–1332.

[15] A. Saffarzadeh, The effects of mn concentration on spin-polarized transport through ZnSe/ZnMnSe/ZnSe heterostructures, Solid State Commun. 137 (2006) 463–468.

[16] W. Xu, Y. Guo, Spin-dependent transport in diluted-magnetic-semiconductor/semiconductor quantum wires, J. Appl. Phys. 100 (2006) 033901.

[17] J.-Q. Lu, Y. Guo, F. Zhai, B.-L. Gu, J.-Z. Yu, Y. Kawazoe, Spin-polarized transport through a magnetic heterostructure: tunneling and spin filtering effect, Phys. Lett. A 299 (2002) 616–621.

[18] X.G. Guo, J.C. Cao, A fully spin-polarized two-dimensional free electron gas induced in narrow diluted magnetic semiconductor quantum wells by in-plane magnetic fields, Semicond. Sci. Technol. 21 (2006) 341.

[19] X.J. Li, K. Chang, Electric-field tuning s-d exchange interaction in quantum dots, Appl. Phys. Lett. 92 (2008) 071116.

[20] K. Chang, S.S. Li, J.B. Xia, F.M. Peeters, Electron and hole states in diluted magnetic semiconductor quantum dots, Phys. Rev. B 69 (2004) 235203.

[21] A.J. Peter, K.L.M. Eucharista, Optically induced magnetization in diluted magnetic quantum dots, J. Magn. Magn. Mater. 321 (2009) 402–407.

[22] D. Lalitha, A.J. Peter, C.K. Yoo, Effects of sp-d exchange on a bound polaron and the g-factor of the exciton in a GaMnAs quantum dot, Superlattices Microstruct. 60 (2013) 453–461.

[23] F.V. Kyrychenko, J. Kossut, Diluted magnetic semiconductor quantum dots: an extreme sensitivity of the hole Zeeman splitting on the aspect ratio of the confining potential, Phys. Rev. B 70 (2004) 205317.

[24] T. Tomita, A. Uetake, T. Asahina, K. Kayanuma, A. Murayama, Y. Oka, Spin injection processes in ZnSe-based double quantum dots of diluted magnetic semiconductors, J. Supercond. Nov. Magn. 18 (2005) 405–410.

[25] M. Triki, S.B. Afia, S. Jaziri, Electron states in CdMnSe/ZnSe and in CdSe/ZnMnSe diluted magnetic semiconductor quantum dots, Phys. Stat. Sol. (c) 6 (2009) 845–848.

[26] N. Kim, H. Kim, T.W. Kang, Manipulation of spin states by dipole polarization switching, Appl. Phys. Lett. 91 (2007) 113504.

[27] H. Kim, N. Kim, Manipulation of spin distribution in double quantum disks with external magnetic field, Semicond. Sci. Technol. 24 (2009) 095015.

[28] L. Jiang, X. Liu, Z. Zhang, R. Wang, Manipulating the spin states in a double molecular magnets tunneling junction, Phys. Lett. A 378 (2014) 426–430.

[29] M. Abramowitz, I.A. Stegun, Handbook of Mathematical Functions with Formulas, Graphs, and Mathematical Tables, Dover Publications, New York, 1970.

[30] L.D. Landau, E.M. Lifshitz, Quantum Mechanics (Non-relativistic Theory), third ed., BPC Wheatons Ltd., Exeter, 1977.

6. ผลลัพท์จากโครงการวิจัย

ความรู้ที่ได้จากโครงงานวิจัยนี้สามารถนำไปประยุกต์ใช้กับอุปกรณ์สปินทรอนิคส์ได้เป็นอย่างดีซึ่งโครงงานวิจัยนี้สามารถเขียนบทความเพื่อเผยแพร่ออกมาในวารสารระดับนานาชาติ Superlattices and Microstructures ที่มีค่า Impact Factor 1.979 ได้แก่

A. Amthong, a magnetic quantum dot in a diluted magnetic semiconductor/ semiconductor heterostructure, Superlattices and Microstructures 80 (2015) 72-79. (Impact Factor 1.979)

ภาคผนวก

Elsevier Editorial System(tm) for Superlattices and Microstructures
Manuscript Draft

Manuscript Number: SM14-1006R1

Title: A magnetic quantum dot in a diluted magnetic semiconductor/semiconductor heterostructure

Article Type: Research Article

Keywords: Diluted magnetic semiconductors; Quantum dot; Heterostructure

Corresponding Author: Dr. Attapon Amthong, Ph.D

Corresponding Author's Institution: Naresuan University

First Author: Attapon Amthong

Order of Authors: Attapon Amthong

A magnetic quantum dot in a diluted magnetic semiconductor/semiconductor heterostructure

Attapon Amthong
Department of Physics, Faculty of Science, Naresuan University, Phitsanulok 65000, Thailand
Email: attapona@nu.ac.th
Tel: +66831652961

A diluted magnetic semiconductor (DMS) is a compound semiconductor formed by doping of a nonmagnetic semiconductor (NMS) by magnetic ions. Magnetic properties in a DMS caused by the impurities have attracted much attention. In a paramagnetic DMS, an external magnetic field gives rise to not only the normal Zeeman splitting but also the strong exchange interaction between band electrons in a DMS and those associated with magnetic ions. As a result, the energy splitting is extremely enhanced. This phenomenon can be interpreted by introducing the effective g-factor which is much larger than the g-factor of band electrons. Experimental studies show the value of the effective g-factor can be tuned to several hundreds, depending upon magnetic concentration, temperature, and host semiconductors.

In this work, a circular quantum dot consisting of a diluted magnetic semiconductor and a nonmagnetic semiconductor in the presence of a constant magnetic field is theoretically investigated. Electron eigenenergies and eigenstates are calculated using effective mass approximation. We show how the spin up and spin down eigenenergies vary with the effective g-factor. Spin-dependent distribution of electron wavefunctions is found. The approximation of the eigenenergies is also discussed.

Suggested reviewers

Dr Simon Crampin
University of Bath
s.crampin@bath.ac.uk

Professor James Annett
University of Bristol
james.annett@bristol.ac.uk

Mouna Triki
Laboratoire de Physique de la Matière Condensée, Faculté des Sciences de Tunis
mounasellami@yahoo.fr

Professor Sihem Jaziri
University of Carthage, Faculty of Sciences
sihem.jaziri@fsb.rnu.tn

Nammee Kim
Soongsil University
nammee@ssu.ac.kr

Thank you for your suggestion. These are your recommendations and my responses.

* In eqn. (3), I would have thought that {1-\Theta(r-R)} is better as \Theta(R-r).

- I agree with you. It has been changed to \Theta(R-r) now.

* In (3), the conventional Zeeman interaction is ignored for r<R; worth explicitly stating?

- In fact, it is the conventional Zeeman interaction outside the dot region (r>R) that is ignored, so I add the below sentence in the paragraph under eq. 3.

" Here, the conventional Zeeman interaction outside the dot region $(r \geq R)$ is vanishingly small, compared to the giant Zeeman interaction existing inside."

* In discussing the solution of (7), the behaviour of \psi_{nm}^\sigma for x -> infinity is surely irrelevant, since this equation only applies for x up to R^2/(2\ell^2).

- You are right. I should not focus on x->infinity because the eq is for x< R^2/(2\ell^2). However, I actually want to discuss the general solution of the Schrodinger equation which is the solution for the region both inside and outside the dot. For this reason, considering both x -> infinity and x-> 0 is necessary.

I am sorry about the process of solving the Schrodinger equation.
It is not well presented. The reader may be confused about it.

In fact, I firstly solve the Schrodinger equation both inside and outside the dot at the same time, and then find the general solution for the region both inside and outside the dot. Finally, the particular solutions inside and outside are considered separately.

When I want to find the general solution, I need to consider the behaviour of the wavefunction when x -> infinity and x->0 to get the solution shown in eq (9) (in the revised manuscript). Note that it is the general solution for the region both inside and outside the dot. The process of solving the Schrodinger equation presented here is very similar to the way we solve the problem of an electron in a uniform magnetic field which can be seen in ref 30.

After that, I find the particular solution inside by substituting the general solution in eq (9) into the Schrodinger equation (7) to obtain the solution in the form of a Kummer-M function and a Kummer-U function. Because I want to find the solution inside, considering the solution when x->0 is necessary. Finally, I get a Kummer-M function as the solution inside.

For the particular solution outside, I again substitute the general solution in eq (9) into the Schrodinger equation (7) to obtain the solution in the form of a Kummer-M function and a Kummer-U function. In this case, I consider the solution when x->infinity to get a Kummer-U function as the solution outside.

In order to correct the process of solving the Schrodinger equation, some eqs. need to be modified in the following.

1. The Heaviside step functions are inserted in eqs (5) and (6) to show that they are the Schrodinger equation for the region both inside and outside the dot.
2. In eq (7) \beta_{\sigma } is changed to \beta_{x}
3. Eq (8) is inserted in the revised manuscript.

A few sentences between eq (4) and eq (12) are also inserted in the following.

1. Between eq (4) and eq (5) in the revised manuscript, I insert

"After substituting the wavefunction (\ref{4}) into the Schr$\ddot{\mathrm{o}}$dinger equation and using the relation $\sigma_{z} \chi_{\sigma}=\sigma \chi_{\sigma}$ where σ is 1 and -1 for spin up and spin down respectively, we obtain the radial equation"

2. Between eq (9) and eq (10) in the revised manuscript, I insert

"To find the solution inside the quantum dot $(r<R)$ where $\beta (x)=\beta _{\sigma }$, we substitute the wavefunction (9) into the Schr$\ddot{\mathrm{o}}$dinger equation (7) and yield the Kummer's equation"

3. Between eq (11) and eq (12) in the revised manuscript, I insert

"Outside the quantum dot region ($r \geq R$) where the giant Zeeman interaction vanishes, we can find the solution in the same way we did before."

* In (10), B is a poor choice for the coefficient since it has meaning elsewhere as the magnetic field.

-In the revised manuscript, A and B have been changed to C_1 and C_2 respectively.

* In the discussion following (10), it is not sufficient to dismiss U because it goes to infinity when x approaches zero, as the full wave function also includes a factor x^{|m|/2} which goes to zero for |m|>0. The argument needs to be made on the behaviour of the product.

-I agree with you. The reason that we can dismiss U is that
" x^{\left | m \right |/2} e^{-x/2} U(\frac{\left | m \right |}{2}+\frac{1}{2}-\beta_{\sigma },\left | m \right |+1,x) diverges when x approaches 0" as you can see in the revised manuscript.

* In line 72, half tesla should be written 0.5 T.

-It has been changed to 0.5 T now.

* In line 110: the magnetic field is uniform everywhere. It is the coupling to the spin that varies spatially.

-I am sorry. I miss some sentences in the line.

In the paragraph, I try to explain why both spin up and spin down states with large angular momentum m behave like Landau states. Because the wavefunctions with large angular momentum m extend far from the origin. Electrons corresponding to the wavefunctions will travel outside the dot region where the magnetic field is uniform and the Zeeman potential is zero. They do not feel the discontinuous Zeeman potential. Consequently, their eigenenergies and eigenstates are similar to Landau levels and Landau states respectively.

On the other hand, the wavefunctions with small angular momentum m extend over the region both inside and outside the dot. Electrons corresponding to the wavefunctions can feel the discontinuous Zeeman potential. In this case, the potential will play a key role in electron confinement and make their eigenenergies differ from the Landau levels.

In the revised manuscript, the below sentences are inserted in the paragraph.

"In a classical viewpoint, electrons corresponding to the states with large $\left | m \right |$ will travel outside the dot region where the magnetic field is uniform and the Zeeman potential is zero. They do not feel the discontinuous Zeeman potential. "

* There is a loss of capitals in some article titles in the references (e.g. gamnas -> GaMnAs).

-Sorry about that. They have been corrected now.

Highlights.

-A DMS/NMS quantum dot is theoretically studied.

- The effective mass approximation is used.

-The effects of the giant Zeeman splitting are investigated.

-The spin-dependent distribution of spin states is found.

A magnetic quantum dot in a diluted magnetic semiconductor/semiconductor heterostructure

A. Amthong[a,b]

[a]*Department of Physics, Faculty of Science, Naresuan University, Phitsanulok 65000, Thailand*
[b]*Research Center for Academic Excellence in Applied Physics, Naresuan University, Phitsanulok 65000, Thailand*

Abstract

A circular quantum dot consisting of a diluted magnetic semiconductor and a nonmagnetic semiconductor in the presence of a constant magnetic field is theoretically investigated. Electron eigenenergies and eigenstates are calculated using effective mass approximation. We show how the spin up and spin down eigenenergies vary with the effective g-factor. Spin-dependent distribution of electron wavefunctions is found. The approximation of the eigenenergies is also discussed.

Keywords: Diluted magnetic semiconductors, Quantum dot, Heterostructure

1. Introduction

A diluted magnetic semiconductor (DMS) [1, 2, 3] is a compound semiconductor formed by doping of a nonmagnetic semiconductor (NMS) by magnetic ions. Magnetic properties in a DMS caused by the impurities have attracted much attention. In a paramagnetic DMS, an external magnetic field gives rise to not only the normal Zeeman splitting but also the strong exchange interaction between band electrons in a DMS and those associated with magnetic ions. As a result, the energy splitting is extremely enhanced. This phenomenon can

☆Fully documented templates are available in the elsarticle package on CTAN.
*Corresponding author
Email address: attaponа@nu.ac.th (A. Amthong)
URL: www.elsevier.com (A. Amthong)

be interpreted by introducing the effective g-factor (g_{eff}) which is much larger than the g-factor of band electrons. Experimental studies show the value of g_{eff} can be tuned to several hundreds, depending upon magnetic concentration, temperature, and host semiconductors [4, 5].

According to the giant Zeeman effect, a DMS has become one of the most potential materials for spintronic application which aims to manipulate spin and charge of carriers [6, 7]. One example of the application is spin polarised bound states which are created in a DMS layer in the presence of nonhomogeneous magnetic fields associated with permalloy disks, Abrikosov vortices, and Josephson vortices [8, 9, 10]. When g_{eff} is sufficiently large, the Zeeman energy will become a major confinement potential, while the potential due to a magnetic vector potential can be neglected. The energy spectrum of the Zeeman-bound states is therefore found to be influenced by magnetic field profiles.

Another possibility is to use a DMS as a tunnel junction. It was first investigated by Egues [11] who focused on the ZnSe/ZnMnSe/ZnSe heterostructure. Based on the concept that spin up and spin down electrons feel different potentials in the region of a DMS, a spin-polarized current can be achieved after injected electrons tunnel through a DMS. Using the different method, Chang and Peeters [12] revisited the problem to support the work of Egues. They additionally investigated the effect of the DMS thickness on spin-dependent conductivity. In the other studies of the heterostructure [13, 14, 15], the effects of the Mn concentration, conduction band offset, and applied electric field are included to improve the spin polarization. The results from related systems consisting of DMSs also show the possibility of spin-polarized tunnelling [16, 17, 18].

Moreover, DMSs are applied to quantum dots. They have been studied for different geometries: a cylinder, a sphere, and a cuboid [19, 20, 21, 22, 23, 24]. Interestingly, Triki [25] proposed the quantum dot heterostructure which is formed by CdMnSe (CdSe) in the shape of a truncated cone surrounded by ZnSe (ZnMnSe) and numerically studied the variation of electron energies as a function of a magnetic field. In the heterostructure, the potential due to

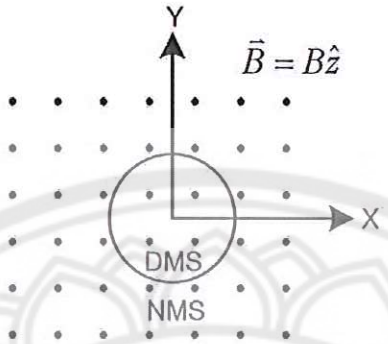

Figure 1: The hybrid system of a circular DMS surrounded by a NMS in a uniform magnetic field $\vec{B} = B\hat{z}$ represented by the symbol •.

the band offset, which is discussed intensively, plays a major role in electron confinement while the giant Zeeman potential only leads to energy splitting of spin up and spin down states.

In this work, we analytically investigate the DMS/NMS quantum dot formed by a disk-shaped DMS surrounded by a NMS as depicted in Fig. 1, focusing on the effect of the giant Zeeman potential. To see the effect clearly, we study the quantum dot where a host semiconductor of a DMS is the same material as a surrounding NMS. In this heterostructure, only the confinement due to the giant Zeeman potential exists while the band offset at the interface can be ignored. The spin-dependent energy spectrum and distribution of electron states are discussed and classified. Without the band offset, we find spin up and spin down states exhibit completely different spatial distribution. These behaviors of spin states may be useful for the application of spin-based memories or future spintronic devices [26, 27, 28].

2. Theoretical formulations

Within the mean field approximation, the potential energy of a conduction band electron travelling in a DMS subjected to a magnetic field $\vec{B} = B\hat{z}$ is given

by

$$V = \frac{1}{2} g^* \mu_B \sigma_z B - \frac{1}{2} N_0 \alpha x \langle S_z \rangle \sigma_z, \tag{1}$$

where the first term is the Zeeman splitting energy and the second one is the potential associated with the exchange interaction between electrons in the conduction band and those of doped magnetic ions. In this equation, g^* is the electron g-factor, σ_z is the z component of Pauli matrices, $N_0\alpha$ is the exchange constant, x is magnetic concentration, and $\langle S_z \rangle$ is the average spin per magnetic site. Because $\langle S_z \rangle$ only exists when a magnetic field is non-vanishing. It is more convenient to write the potential as

$$V = -\frac{1}{2} g_{\text{eff}} \mu_B \sigma_z B, \tag{2}$$

where $g_{\text{eff}} = -g^* + \frac{N_0 \alpha x \langle S_z \rangle}{\mu_B B}$ is the effective g-factor [8].

In our study, the layer of DMS/NMS heterostructure placed on $x - y$ plane in the presence of a magnetic field $\vec{B} = B\hat{z}$ is investigated. For simplicity, we assume that electrons move effectively in the plane. Within the effective mass approximation, the Hamiltonian in cylindrical coordinates (r, ϕ, z) describing a single electron $(q = -e)$ in the layer is

$$\widehat{H} = \frac{(\hat{p} + e\vec{A})^2}{2M} - \frac{1}{2} g_{\text{eff}} \mu_B \sigma_z B \Theta(R - r), \tag{3}$$

where M is the effective mass of an electron, R is the radius of a circular DMS, and Θ is the Heaviside step function. Here, the conventional Zeeman interaction outside the dot region $(r \geq R)$ is vanishingly small, compared to the giant Zeeman interaction existing inside. The symmetric gauge $\vec{A} = (Br/2)\hat{\phi}$ is chosen in our calculation. Due to the rotational symmetry of the Hamiltonian, the general form of the eigenfunction can be expressed as

$$\Psi^{\sigma}_{nm}(r, \phi) = e^{im\phi} \psi^{\sigma}_{nm}(r) \chi_{\sigma}, \tag{4}$$

where n, m, and σ refer to a radial quantum number, an angular momentum and spin ($\uparrow$ or $\downarrow$) respectively. $\chi_{\uparrow\downarrow}$ is the column matrix representing a spin up $\binom{1}{0}$ or spin down $\binom{0}{1}$ state. After substituting the wavefunction (4) into the

Schrödinger equation and using the relation $\sigma_z\chi_\sigma = \sigma\chi_\sigma$ where σ is 1 and -1 for spin up and spin down respectively, we obtain the radial equation

$$-\frac{\hbar^2}{2M}\left(\frac{\partial^2}{\partial r^2}+\frac{1}{r}\frac{\partial}{\partial r}-\frac{m^2}{r^2}\right)\psi^\sigma_{nm}(r)+\left(\frac{m\hbar\omega_c}{2}+\frac{M\omega_c^2 r^2}{8}\right)\psi^\sigma_{nm}(r) - \left(\frac{\sigma g_{\text{eff}}\mu_B B\Theta(R-r)}{2}\right)\psi^\sigma_{nm}(r) = E\psi^\sigma_{nm}(r), \quad (5)$$

where $\omega_c = eB/M$ is the cyclotron frequency. We then measure all of the quantities in the following units: $r = \rho\ell$, $E = \epsilon\hbar\omega_c$, and $M = m^*M_e$ where $\ell = \sqrt{\hbar/eB}$ is the magnetic length and M_e is the electron rest mass. The Schrödinger equation is rewritten in the dimensionless form

$$\left(-\frac{1}{2}\frac{\partial^2}{\partial\rho^2}-\frac{1}{2\rho}\frac{\partial}{\partial\rho}+\frac{m^2}{2\rho^2}+\frac{m}{2}+\frac{\rho^2}{8}-\frac{\sigma g_{\text{eff}}m^*\Theta(R/\ell-\rho)}{4}\right)\psi^\sigma_{nm}(\rho)=\epsilon\psi^\sigma_{nm}(\rho). \quad (6)$$

After that, we define another variable $x = \rho^2/2$. The Schrödinger equation now becomes

$$\left(x\frac{\partial^2}{\partial x^2}+\frac{\partial}{\partial x}-\frac{x}{4}-\frac{m^2}{4x}+\beta(x)\right)\psi^\sigma_{nm}(x)=0, \quad (7)$$

where

$$\beta(x)=\begin{cases}\beta_\sigma & x < R^2/(2\ell^2)\\ \beta_0 & x \geq R^2/(2\ell^2),\end{cases} \quad (8)$$

$\beta_\sigma = \beta_0 + (\sigma g_{\text{eff}}m^*/4)$, and $\beta_0 = \epsilon - m/2$. Considering the solutions when x is close to 0 and infinity, we find the wavefunction $\psi^\sigma_{nm}(x)$ can be expressed as $\psi^\sigma_{nm}(x\to 0) = x^{|m|/2}$ and $\psi^\sigma_{nm}(x\to\infty) = e^{-x/2}$. Therefore, the general solution of the Eq. (7) is given by

$$\psi^\sigma_{nm}(x) = x^{|m|/2}e^{-x/2}w(x). \quad (9)$$

To find the solution inside the quantum dot ($r < R$) where $\beta(x) = \beta_\sigma$, we substitute the wavefunction (9) into the Schrödinger equation (7) and yield the Kummer's equation [29]

$$x\frac{\partial^2 w}{\partial x^2}+(|m|+1-x)\frac{\partial w}{\partial x}-(\frac{|m|}{2}+\frac{1}{2}-\beta_\sigma)w=0, \quad (10)$$

whose solution is

$$w(x) = C_1M(\frac{|m|}{2}+\frac{1}{2}-\beta_\sigma,|m|+1,x)+C_2U(\frac{|m|}{2}+\frac{1}{2}-\beta_\sigma,|m|+1,x), \quad (11)$$

where C_1 and C_2 are arbitrary constants. M and U are a Kummer-M function and Kummer-U function respectively. Because $x^{|m|/2}e^{-x/2}U(\frac{|m|}{2}+\frac{1}{2}-\beta_\sigma, |m|+1, x)$ diverges when x approaches 0, we choose $C_2 = 0$ to obtain a Kummer-M function as the solution inside the quantum dot.

Outside the quantum dot region ($r \geq R$) where the giant Zeeman interaction vanishes, we can find the solution in the same way we did before. In this case, we also get the solution in the form of a Kummer-M function and Kummer-U function as shown in the Eq. (11), but β_σ is replaced by β_0. When x approaches infinity, a Kummer-M function $M(\frac{|m|}{2}+\frac{1}{2}-\beta_0, |m|+1, x)$ is proportional to $e^x x^{(-\frac{|m|}{2}-\frac{1}{2}-\beta_0)}$. This causes the wavefunction $\psi^\sigma_{nm}(x)$ to diverge. Hence, we choose $C_1 = 0$ in this case to get a Kummer-U function as the solution outside the quantum dot. The radial wavefunction corresponding to the Schrödinger equation (6) is expressed in term of ρ as

$$\psi^\sigma_{nm}(\rho) = \begin{cases} C_1 e^{-\rho^2/4}\rho^{|m|}M(-a_1, b, \rho^2/2) & \rho < \sqrt{2s} \\ C_2 e^{-\rho^2/4}\rho^{|m|}U(-a_2, b, \rho^2/2) & \rho \geq \sqrt{2s}, \end{cases} \tag{12}$$

where $a_1 = \beta_\sigma - |m|/2 - 1/2$, $a_2 = \beta_0 - |m|/2 - 1/2 = a_1 - \sigma g_{\text{eff}} m^*/4$, and $b = |m|+1$. s is the dimensionless parameter defined by $s = B\pi R^2/(h/e) = \Phi/\Phi_0$; $\Phi = B\pi R^2$ and $\Phi_0 = h/e$. It determines the magnetic flux Φ passing through the quantum dot region in the unit of the flux quantum Φ_0. At the edge of the dot where $r = R$, we have the corresponding $\rho = \sqrt{2s}$. Now, C_1 and C_2 are constants satisfying the normalization condition $\int_0^{2\pi}\int_0^\infty \Psi^*\Psi r dr d\phi = 1$. From the definition of a_1, the eigenenergy can be expressed as

$$\epsilon^\sigma_{nm} = a_1 + \frac{m}{2} + \frac{|m|}{2} + \frac{1}{2} - \frac{\sigma g_{\text{eff}} m^*}{4}. \tag{13}$$

To find the values of a_1, we match the radial wavefunctions inside and outside the quantum dot by the boundary condition, i.e., the logarithmic derivatives of the wavefunctions at the dot radius ($\rho = \sqrt{2s}$)

$$\frac{\mathrm{d}}{\mathrm{d}\rho}\ln\psi^{in}(\rho)\Big|_{\rho=\sqrt{2s}} = \frac{\mathrm{d}}{\mathrm{d}\rho}\ln\psi^{out}(\rho)\Big|_{\rho=\sqrt{2s}}. \tag{14}$$

This Eq. leads to

$$a_1 - a_1\frac{M(1-a_1, b, s)}{M(-a_1, b, s)} = a_2 + a_2(a_2+b-1)\frac{U(1-a_2, b, s)}{U(-a_2, b, s)}, \tag{15}$$

which can be solved numerically to obtain the quantized values of a_1.

When g_{eff} is extremely large, it is obvious that the giant Zeeman potential $-\sigma g_{\text{eff}} m^*/4$ in Eq. (6) will greatly lower the energy levels of spin up states $\psi^{\uparrow}_{nm}(\rho)$. Then, the states are strongly confined in a very deep quantum well which is formed by the Zeeman potential existing inside the dot region. In this circumstance, we could assume that the spin up wavefunctions only distribute inside the dot region and vanish at the dot radius. With this approximation, the wavefunctions in Eq. (12) for spin up states become

$$\psi^{\uparrow}_{nm}(\rho) = Ae^{-\rho^2/4}\rho^{|m|}M(-a_1, b, \rho^2/2), \tag{16}$$

where $\psi^{\uparrow}_{nm}(\rho = \sqrt{2s}) = 0$. This boundary condition leads to

$$M(-\beta_\sigma + \frac{|m|}{2} + \frac{1}{2}, |m| + 1, s) = 0. \tag{17}$$

Defining α^M_n as the n^{th} zero of the Kummer-M function, which satisfies $M(\alpha^M_n, |m|+1, s) = 0$, we obtain the approximated eigenenergies $(\epsilon^{\uparrow}_{app})$ corresponding to the spin up states

$$\epsilon^{\uparrow}_{app} = -\alpha^M_n + \frac{m}{2} + \frac{|m|}{2} + \frac{1}{2} - \frac{g_{\text{eff}} m^*}{4}. \tag{18}$$

Conversely, the giant Zeeman potential $-\sigma g_{\text{eff}} m^*/4$ will act as a very high barrier for spin down states, which does not allow the states to enter the dot region. In this case, we could assume that the spin down wavefunctions only distribute outside the dot region and vanish at the dot radius to get

$$\psi^{\downarrow}_{nm}(\rho) = Be^{-\rho^2/4}\rho^{|m|}U(-a_2, b, \rho^2/2), \tag{19}$$

where $\psi^{\downarrow}_{nm}(\rho = \sqrt{2s}) = 0$. This boundary condition leads to

$$U(-\beta_0 + \frac{|m|}{2} + \frac{1}{2}, |m| + 1, s) = 0. \tag{20}$$

Defining α^U_n as the n^{th} zero of the Kummer-U function, which satisfies $U(\alpha^U_n, |m|+1, s) = 0$, we obtain the approximated eigenenergies $(\epsilon^{\downarrow}_{app})$ corresponding to the spin down states

$$\epsilon^{\downarrow}_{app} = -\alpha^U_n + \frac{m}{2} + \frac{|m|}{2} + \frac{1}{2}. \tag{21}$$

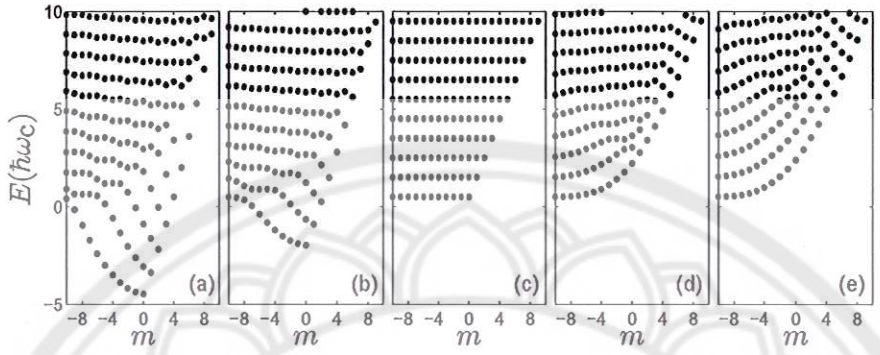

Figure 2: The energy spectrum of spin up and spin down eigenstates for various values of g_{eff}. (a) $E^{\uparrow}$ with $g_{\text{eff}} = 40$, (b) $E^{\uparrow}$ with $g_{\text{eff}} = 20$, (c) $E^{\uparrow}$ and $E^{\downarrow}$ with $g_{\text{eff}} = 0$, (d) $E^{\downarrow}$ with $g_{\text{eff}} = 20$, and (e) $E^{\downarrow}$ with $g_{\text{eff}} = 40$.

3. Results and discussion

After solving Eq. (15) numerically, we obtain the quantized values of a_1 for spin up and spin down states, leading to the spin-dependent eigenenergies in Eq. (13) as shown in Fig. 2. In this calculation, $m^* = 0.5$ and $s = 4$, corresponding to a quantum dot radius $R = 100$ nm and a magnetic field of 0.5 T. To see the effect of the giant Zeeman potential clearly, the value of g_{eff} is varied in each panel of the figure. Note that g_{eff} can be controlled by temperature, magnetic concentration, and host semiconductors in experiments.

Without the Zeeman potential ($g_{\text{eff}} = 0$), spin up and spin down states have the same energies as seen in Fig. 2(c). Because electrons only feel a uniform magnetic field, their energy levels are exactly the same as the well-known Landau levels [30]: $\epsilon = n + m/2 + |m|/2 + 1/2$. When g_{eff} is greater than zero, electrons additionally feel the discontinuous Zeeman potential. This leads to the energy spectrum which can be considered as Landau levels disturbed by the exchange interaction in a DMS region.

In Fig. 2(a) and (b), we see that some low-lying energy levels of spin up states tend to separate from the others with increasing of g_{eff}, resulting in two

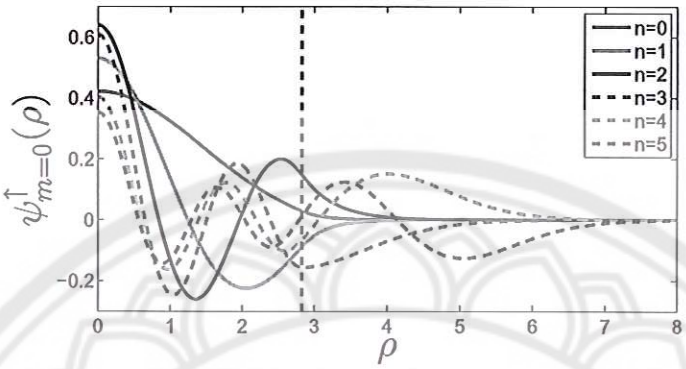

Figure 3: Spin up radial wavefunctions with $m = 0$ corresponding to the eigenenergies in Fig. 2(a) where $g_{\text{eff}} = 40$. The black dashed line represents the dot radius where $\rho = \sqrt{8}$.

energy patterns concerning the distribution of wavefunctions. Examples of low-lying states represented by solid lines are shown in Fig. 3. Their energies are negative because the negative Zeeman potential $-g_{\text{eff}}m^*/4$ in Eq. (6) behaves like a quantum well to trap the states. For this reason, they are mostly localized inside the dot region and start decaying when extending outside. The high-energy excited states represented by dashed lines behave differently. Due to their positive energies, they are not confined by the Zeeman quantum well. As seen in Fig. 3, the states oscillate over the region both inside and outside the dot.

In the case of the spin down spectrum shown in Fig. 2(d) and (e), the Zeeman potential $g_{\text{eff}}m^*/4$ existing in the DMS region will act as a barrier to perturb Landau levels by raising the energy levels. We find low-lying states are pushed by the Zeeman barrier to the region outside. As seen in Fig. 4, the states with $n = 0, 1$, and 2 oscillate outside and decay when extending inside the dot region. If energies of excited states are greater than the Zeeman potential $g_{\text{eff}}m^*/4$, they will be able to extend over the region both inside and outside the dot. As seen in the figure, the states $\psi^{\downarrow}_{n=3,4,5}$ with energies 5.606, 6.095, and 7.099 can oscillate in the DMS region, where the Zeeman potential in the figure is $g_{\text{eff}}m^*/4 = 5$. Note that all energies are in the unit of $\hbar\omega_c$. Raising the value

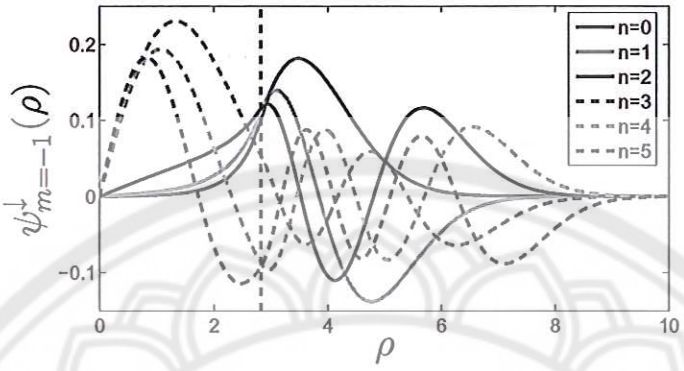

Figure 4: Spin down radial wavefunctions with $m = -1$ corresponding to the eigenenergies in Fig. 2(e) where $g_{\text{eff}} = 40$. The black dashed line represents the dot radius where $\rho = \sqrt{8}$

of g_{eff} will increase the number of the states which decay inside the dot region.

When $|m|$ is sufficiently large, both spin up and spin down states will behave like Landau states. Considering Eq. (6), one can see that the term $m^2/2\rho^2$ acts as a barrier which does not allow wavefunctions to enter the center of the quantum dot. As a result, the wavefunctions with large $|m|$ will extend far from the origin. In a classical viewpoint, electrons corresponding to the states with large $|m|$ will travel outside the dot region where the magnetic field is uniform and the Zeeman potential is zero. They do not feel the discontinuous Zeeman potential. Consequently, their eigenenergies and eigenstates are similar to Landau levels and Landau states respectively.

Fig. 5 shows the approximated eigenenergies of spin up and spin down states in the circumstance where the giant Zeeman potential is extremely large (g_{eff}=500). We find that our spin up approximation agrees well with the eigenenergies of low-lying states with small $|m|$. This is because the spatial distribution of high energy states and the states with large $|m|$ is not consistent with the assumption in our approximation; they can penetrate deep into the region outside. On the other hand, the approximated eigenenergies of spin down states are found to be in good agreement when $|m|$ is sufficiently large. For each value of m, we see that the energies of excited states tend to differ from approximated

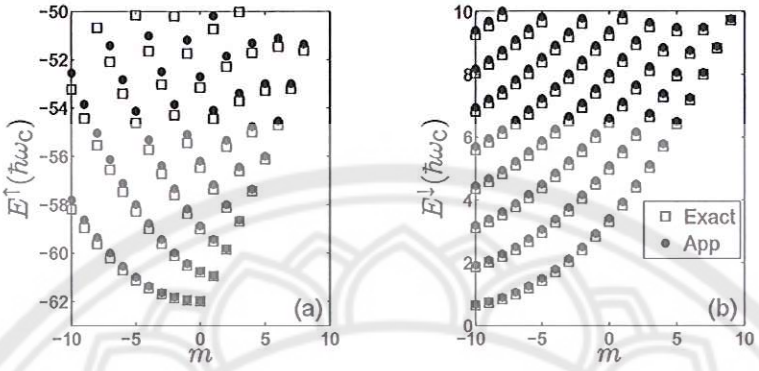

Figure 5: Comparison of exact eigenenergies (squares) and approximated energies (points) when g_{eff} is 500, $s = 6$, and $m^* = 0.5$ for (a) spin up and (b) spin down.

values. This is because these states can penetrate deep into the dot region.

In conclusion, we have presented the quantum dot heterostructure of a DMS and a NMS in the presence of a uniform magnetic field, where a band offset at a mismatched interface is vanishingly small, compared to the giant Zeeman splitting. Spin-dependent eigenenergies and eigenstates describing electrons trapped in the quantum dot are derived by matching wavefunctions at the boundary. It is found that the Zeeman potential due to the exchange interaction in a DMS can be used to control the spin distribution of low-lying states. That is, spin up states are confined inside the dot region, while spin down states extend outside. If energies of spin states are sufficiently large, they will be able to distribute over the region both inside and outside the dot. These results may be useful for manipulating spin states in spintronic application. However, for the heterostructure where a band offset is significant the spin-dependent localization will not be found. We also calculate the approximated eigenenergies when g_{eff} is very large. Good approximation is found when spin up wavefunctions are strongly localized inside the dot area and spin down wavefunctions overwhelmingly distribute outside.

4. Acknowledgements

This work was financially supported by Naresuan University Research Grants.

References

References

[1] J. K. Furdyna, Diluted magnetic semiconductors: An interface of semiconductor physics and magnetism (invited), J. Appl. Phys. 53 (1982) 7637–7643.

[2] J. K. Furdyna, Diluted magnetic semiconductors, J. Appl. Phys. 64 (1988) R29–R64.

[3] W. de Jonge, H. Swagten, Magnetic properties of diluted magnetic semiconductors, J. Magn. Magn. Mater. 100 (1991) 322–345.

[4] A. Hundt, J. Puls, F. Henneberger, Spin properties of self-organized diluted magnetic Cd_{1-x} Mn_x Se quantum dots, Phys. Rev. B 69 (2004) 121309.

[5] T. Dietl, M. Sawicki, M. Dahl, D. Heiman, E. D. Isaacs, M. J. Graf, S. I. Gubarev, D. L. Alov, Spin-flip scattering near the metal-to-insulator transition in $Cd_{0.95}$ $Mn_{0.05}$ Se:In, Phys. Rev. B 43 (1991) 3154–3163.

[6] P. Kacman, Spin interactions in diluted magnetic semiconductors and magnetic semiconductor structures, Semicond. Sci. Technol. 16 (2001) R25.

[7] I. Žutić, J. Fabian, S. Das Sarma, Spintronics: Fundamentals and applications, Rev. Mod. Phys. 76 (2004) 323–410.

[8] T. G. Rappoport, M. Berciu, B. Jankó, Effect of the Abrikosov vortex phase on spin and charge states in magnetic semiconductor-superconductor hybrids, Phys. Rev. B 74 (2006) 094502.

[9] M. Berciu, B. Jankó, Nanoscale Zeeman localization of charge carriers in diluted magnetic semiconductor-permalloy hybrids, Phys. Rev. Lett. 90 (2003) 246804.

[10] X. L. Wang, C. T. Lin, B. Liang, S. Yu, S. Ooi, K. Hirata, S. Y. Ding, D. Q. Shi, S. X. Dou, Z. W. Lin, J. G. Zhu, Josephson-vortex flow resistance in $Bi_2Sr_2Ca_2Cu_3O_y$ single crystals and its possible application in the manipulation of spin and charge textures in diluted magnetic semiconductors, J. Appl. Phys. 101 (2007) 09G116.

[11] J. C. Egues, Spin-dependent perpendicular magnetotransport through a tunable $ZnSe/Zn_{1-x}Mn_xSe$ heterostructure: A possible spin filter?, Phys. Rev. Lett. 80 (1998) 4578–4581.

[12] K. Chang, F. Peeters, Spin polarized tunneling through diluted magnetic semiconductor barriers, Solid State Commun. 120 (2001) 181 – 184.

[13] Y. Guo, H. Wang, B.-L. Gu, Y. Kawazoe, Spin-polarized transport through a $ZnSe/Zn_{1-x}Mn_xSe$ heterostructure under an applied electric field, J. Appl. Phys. 88 (2000) 6614–6617.

[14] F. Zhai, Y. Guo, B.-L. Gu, Effects of conduction band offset on spin-polarized transport through a semimagnetic semiconductor heterostructure, J. Appl. Phys. 90 (2001) 1328–1332.

[15] A. Saffarzadeh, The effects of mn concentration on spin-polarized transport through ZnSe/ZnMnSe/ZnSe heterostructures, Solid State Commun. 137 (2006) 463 – 468.

[16] W. Xu, Y. Guo, Spin-dependent transport in diluted-magnetic-semiconductor/semiconductor quantum wires, J. Appl. Phys. 100 (2006) 033901.

[17] J.-Q. Lu, Y. Guo, F. Zhai, B.-L. Gu, J.-Z. Yu, Y. Kawazoe, Spin-polarized transport through a magnetic heterostructure: tunneling and spin filtering effect, Phys. Lett. A 299 (2002) 616 – 621.

[18] X. G. Guo, J. C. Cao, A fully spin-polarized two-dimensional free electron gas induced in narrow diluted magnetic semiconductor quantum wells by in-plane magnetic fields, Semicond. Sci. Technol. 21 (2006) 341.

[19] X. J. Li, K. Chang, Electric-field tuning s-d exchange interaction in quantum dots, Appl. Phys. Lett. 92 (2008) 071116.

[20] K. Chang, S. S. Li, J. B. Xia, F. M. Peeters, Electron and hole states in diluted magnetic semiconductor quantum dots, Phys. Rev. B 69 (2004) 235203.

[21] A. J. Peter, K. L. M. Eucharista, Optically induced magnetization in diluted magnetic quantum dots, J. Magn. Magn. Mater. 321 (2009) 402 – 407.

[22] D. Lalitha, A. J. Peter, C. K. Yoo, Effects of sp-d exchange on a bound polaron and the g-factor of the exciton in a GaMnAs quantum dot, Superlattices Microstruct. 60 (2013) 453 – 461.

[23] F. V. Kyrychenko, J. Kossut, Diluted magnetic semiconductor quantum dots: An extreme sensitivity of the hole Zeeman splitting on the aspect ratio of the confining potential, Phys. Rev. B 70 (2004) 205317.

[24] T. Tomita, A. Uetake, T. Asahina, K. Kayanuma, A. Murayama, Y. Oka, Spin injection processes in ZnSe-based double quantum dots of diluted magnetic semiconductors, J. Supercond. Nov. Magn. 18 (2005) 405–410.

[25] M. Triki, S. B. Afia, S. Jaziri, Electron states in CdMnSe/ZnSe and in CdSe/ZnMnSe diluted magnetic semiconductor quantum dots, Phys. Stat. Sol. (c) 6 (2009) 845–848.

[26] N. Kim, H. Kim, T. W. Kang, Manipulation of spin states by dipole polarization switching, Appl. Phys. Lett. 91 (2007) 113504.

[27] H. Kim, N. Kim, Manipulation of spin distribution in double quantum disks with external magnetic field, Semicond. Sci. Technol. 24 (2009) 095015.

[28] L. Jiang, X. Liu, Z. Zhang, R. Wang, Manipulating the spin states in a double molecular magnets tunneling junction, Phys. Lett. A 378 (2014) 426 – 430.

[29] M. Abramowitz, I. A. Stegun, Handbook of mathematical functions with-
220 formulas, graphs, and mathematical tables, Dover Publications, New York, 1970.

[30] L. D. Landau, E. M. Lifshitz, Quantum Mechanics (Non-relativistic Theory), 3 ed., BPC Wheatons Ltd, Exeter, 1977.

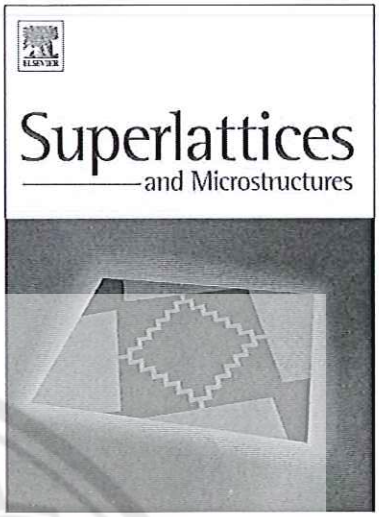

A magnetic quantum dot in a diluted magnetic semiconductor/semiconductor heterostructure

A. Amthong

PII: S0749-6036(15)00003-8
DOI: http://dx.doi.org/10.1016/j.spmi.2014.12.032
Reference: YSPMI 3549

To appear in: *Superlattices and Microstructures*

Received Date: 3 November 2014
Revised Date: 29 December 2014
Accepted Date: 31 December 2014

Please cite this article as: A. Amthong, A magnetic quantum dot in a diluted magnetic semiconductor/semiconductor heterostructure, *Superlattices and Microstructures* (2015), doi: http://dx.doi.org/10.1016/j.spmi.2014.12.032

A magnetic quantum dot in a diluted magnetic semiconductor/semiconductor heterostructure

A. Amthong[a,b]

[a]*Department of Physics, Faculty of Science, Naresuan University, Phitsanulok 65000, Thailand*
[b]*Research Center for Academic Excellence in Applied Physics, Naresuan University, Phitsanulok 65000, Thailand*

Abstract

A circular quantum dot consisting of a diluted magnetic semiconductor and a nonmagnetic semiconductor in the presence of a constant magnetic field is theoretically investigated. Electron eigenenergies and eigenstates are calculated using effective mass approximation. We show how the spin up and spin down eigenenergies vary with the effective g-factor. Spin-dependent distribution of electron wavefunctions is found. The approximation of the eigenenergies is also discussed.

Keywords: Diluted magnetic semiconductors, Quantum dot, Heterostructure

1. Introduction

A diluted magnetic semiconductor (DMS) [1, 2, 3] is a compound semiconductor formed by doping of a nonmagnetic semiconductor (NMS) by magnetic ions. Magnetic properties in a DMS caused by the impurities have attracted much attention. In a paramagnetic DMS, an external magnetic field gives rise to not only the normal Zeeman splitting but also the strong exchange interaction between band electrons in a DMS and those associated with magnetic ions. As a result, the energy splitting is extremely enhanced. This phenomenon can

☆Fully documented templates are available in the elsarticle package on CTAN.

*Corresponding author
Email address: attapona@nu.ac.th (A. Amthong)
URL: www.elsevier.com (A. Amthong)

be interpreted by introducing the effective g-factor (g_{eff}) which is much larger than the g-factor of band electrons. Experimental studies show the value of g_{eff} can be tuned to several hundreds, depending upon magnetic concentration, temperature, and host semiconductors [4, 5].

According to the giant Zeeman effect, a DMS has become one of the most potential materials for spintronic application which aims to manipulate spin and charge of carriers [6, 7]. One example of the application is spin polarised bound states which are created in a DMS layer in the presence of nonhomogeneous magnetic fields associated with permalloy disks, Abrikosov vortices, and Josephson vortices [8, 9, 10]. When g_{eff} is sufficiently large, the Zeeman energy will become a major confinement potential, while the potential due to a magnetic vector potential can be neglected. The energy spectrum of the Zeeman-bound states is therefore found to be influenced by magnetic field profiles.

Another possibility is to use a DMS as a tunnel junction. It was first investigated by Egues [11] who focused on the ZnSe/ZnMnSe/ZnSe heterostructure. Based on the concept that spin up and spin down electrons feel different potentials in the region of a DMS, a spin-polarized current can be achieved after injected electrons tunnel through a DMS. Using the different method, Chang and Peeters [12] revisited the problem to support the work of Egues. They additionally investigated the effect of the DMS thickness on spin-dependent conductivity. In the other studies of the heterostructure [13, 14, 15], the effects of the Mn concentration, conduction band offset, and applied electric field are included to improve the spin polarization. The results from related systems consisting of DMSs also show the possibility of spin-polarized tunnelling [16, 17, 18].

Moreover, DMSs are applied to quantum dots. They have been studied for different geometries: a cylinder, a sphere, and a cuboid [19, 20, 21, 22, 23, 24]. Interestingly, Triki [25] proposed the quantum dot heterostructure which is formed by CdMnSe (CdSe) in the shape of a truncated cone surrounded by ZnSe (ZnMnSe) and numerically studied the variation of electron energies as a function of a magnetic field. In the heterostructure, the potential due to

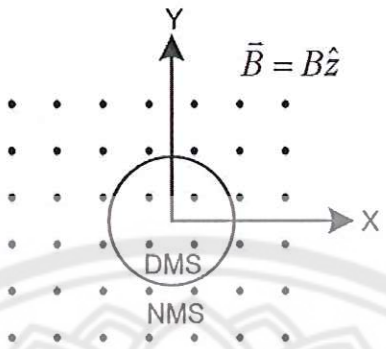

Figure 1: The hybrid system of a circular DMS surrounded by a NMS in a uniform magnetic field $\vec{B} = B\hat{z}$ represented by the symbol •.

the band offset, which is discussed intensively, plays a major role in electron confinement while the giant Zeeman potential only leads to energy splitting of spin up and spin down states.

In this work, we analytically investigate the DMS/NMS quantum dot formed by a disk-shaped DMS surrounded by a NMS as depicted in Fig. 1, focusing on the effect of the giant Zeeman potential. To see the effect clearly, we study the quantum dot where a host semiconductor of a DMS is the same material as a surrounding NMS. In this heterostructure, only the confinement due to the giant Zeeman potential exists while the band offset at the interface can be ignored. The spin-dependent energy spectrum and distribution of electron states are discussed and classified. Without the band offset, we find spin up and spin down states exhibit completely different spatial distribution. These behaviors of spin states may be useful for the application of spin-based memories or future spintronic devices [26, 27, 28].

2. Theoretical formulations

Within the mean field approximation, the potential energy of a conduction band electron travelling in a DMS subjected to a magnetic field $\vec{B} = B\hat{z}$ is given

by

$$V = \frac{1}{2} g^* \mu_B \sigma_z B - \frac{1}{2} N_0 \alpha x \langle S_z \rangle \sigma_z, \tag{1}$$

where the first term is the Zeeman splitting energy and the second one is the potential associated with the exchange interaction between electrons in the conduction band and those of doped magnetic ions. In this equation, g^* is the electron g-factor, σ_z is the z component of Pauli matrices, $N_0\alpha$ is the exchange constant, x is magnetic concentration, and $\langle S_z \rangle$ is the average spin per magnetic site. Because $\langle S_z \rangle$ only exists when a magnetic field is non-vanishing. It is more convenient to write the potential as

$$V = -\frac{1}{2} g_{\text{eff}} \mu_B \sigma_z B, \tag{2}$$

where $g_{\text{eff}} = -g^* + \frac{N_0 \alpha x \langle S_z \rangle}{\mu_B B}$ is the effective g-factor [8].

In our study, the layer of DMS/NMS heterostructure placed on $x-y$ plane in the presence of a magnetic field $\vec{B} = B\hat{z}$ is investigated. For simplicity, we assume that electrons move effectively in the plane. Within the effective mass approximation, the Hamiltonian in cylindrical coordinates (r, ϕ, z) describing a single electron $(q = -e)$ in the layer is

$$\hat{H} = \frac{(\hat{p} + e\vec{A})^2}{2M} - \frac{1}{2} g_{\text{eff}} \mu_B \sigma_z B \Theta(R - r), \tag{3}$$

where M is the effective mass of an electron, R is the radius of a circular DMS, and Θ is the Heaviside step function. Here, the conventional Zeeman interaction outside the dot region $(r \geq R)$ is vanishingly small, compared to the giant Zeeman interaction existing inside. The symmetric gauge $\vec{A} = (Br/2)\hat{\phi}$ is chosen in our calculation. Due to the rotational symmetry of the Hamiltonian, the general form of the eigenfunction can be expressed as

$$\Psi^{\sigma}_{nm}(r, \phi) = e^{im\phi} \psi^{\sigma}_{nm}(r) \chi_{\sigma}, \tag{4}$$

where n, m, and σ refer to a radial quantum number, an angular momentum and spin ($\uparrow$ or $\downarrow$) respectively. $\chi_{\uparrow\downarrow}$ is the column matrix representing a spin up $\binom{1}{0}$ or spin down $\binom{0}{1}$ state. After substituting the wavefunction (4) into the

Schrödinger equation and using the relation $\sigma_z\chi_\sigma = \sigma\chi_\sigma$ where σ is 1 and -1 for spin up and spin down respectively, we obtain the radial equation

$$-\frac{\hbar^2}{2M}\left(\frac{\partial^2}{\partial r^2}+\frac{1}{r}\frac{\partial}{\partial r}-\frac{m^2}{r^2}\right)\psi^\sigma_{nm}(r)+\left(\frac{m\hbar\omega_c}{2}+\frac{M\omega_c^2 r^2}{8}\right)\psi^\sigma_{nm}(r) - \left(\frac{\sigma g_{\rm eff}\mu_B B\Theta(R-r)}{2}\right)\psi^\sigma_{nm}(r) = E\psi^\sigma_{nm}(r), \quad (5)$$

where $\omega_c = eB/M$ is the cyclotron frequency. We then measure all of the quantities in the following units: $r = \rho\ell$, $E = \epsilon\hbar\omega_c$, and $M = m^*M_e$ where $\ell = \sqrt{\hbar/eB}$ is the magnetic length and M_e is the electron rest mass. The Schrödinger equation is rewritten in the dimensionless form

$$\left(-\frac{1}{2}\frac{\partial^2}{\partial\rho^2}-\frac{1}{2\rho}\frac{\partial}{\partial\rho}+\frac{m^2}{2\rho^2}+\frac{m}{2}+\frac{\rho^2}{8}-\frac{\sigma g_{\rm eff}m^*\Theta(R/\ell-\rho)}{4}\right)\psi^\sigma_{nm}(\rho)=\epsilon\psi^\sigma_{nm}(\rho). \quad (6)$$

After that, we define another variable $x = \rho^2/2$. The Schrödinger equation now becomes

$$\left(x\frac{\partial^2}{\partial x^2}+\frac{\partial}{\partial x}-\frac{x}{4}-\frac{m^2}{4x}+\beta(x)\right)\psi^\sigma_{nm}(x)=0, \quad (7)$$

where

$$\beta(x)=\begin{cases}\beta_\sigma & x < R^2/(2\ell^2)\\ \beta_0 & x \geq R^2/(2\ell^2),\end{cases} \quad (8)$$

$\beta_\sigma = \beta_0 + (\sigma g_{\rm eff}m^*/4)$, and $\beta_0 = \epsilon - m/2$. Considering the solutions when x is close to 0 and infinity, we find the wavefunction $\psi^\sigma_{nm}(x)$ can be expressed as $\psi^\sigma_{nm}(x\to 0) = x^{|m|/2}$ and $\psi^\sigma_{nm}(x\to\infty) = e^{-x/2}$. Therefore, the general solution of the Eq. (7) is given by

$$\psi^\sigma_{nm}(x) = x^{|m|/2}e^{-x/2}w(x). \quad (9)$$

To find the solution inside the quantum dot ($r < R$) where $\beta(x) = \beta_\sigma$, we substitute the wavefunction (9) into the Schrödinger equation (7) and yield the Kummer's equation [29]

$$x\frac{\partial^2 w}{\partial x^2}+(|m|+1-x)\frac{\partial w}{\partial x}-(\frac{|m|}{2}+\frac{1}{2}-\beta_\sigma)w=0, \quad (10)$$

whose solution is

$$w(x) = C_1M(\frac{|m|}{2}+\frac{1}{2}-\beta_\sigma,|m|+1,x)+C_2U(\frac{|m|}{2}+\frac{1}{2}-\beta_\sigma,|m|+1,x), \quad (11)$$

where C_1 and C_2 are arbitrary constants. M and U are a Kummer-M function and Kummer-U function respectively. Because $x^{|m|/2}e^{-x/2}U(\frac{|m|}{2}+\frac{1}{2}-\beta_\sigma, |m|+1, x)$ diverges when x approaches 0, we choose $C_2 = 0$ to obtain a Kummer-M function as the solution inside the quantum dot.

Outside the quantum dot region ($r \geq R$) where the giant Zeeman interaction vanishes, we can find the solution in the same way we did before. In this case, we also get the solution in the form of a Kummer-M function and Kummer-U function as shown in the Eq. (11), but β_σ is replaced by β_0. When x approaches infinity, a Kummer-M function $M(\frac{|m|}{2}+\frac{1}{2}-\beta_0, |m|+1, x)$ is proportional to $e^x x^{(-\frac{|m|}{2}-\frac{1}{2}-\beta_0)}$. This causes the wavefunction $\psi^\sigma_{nm}(x)$ to diverge. Hence, we choose $C_1 = 0$ in this case to get a Kummer-U function as the solution outside the quantum dot. The radial wavefunction corresponding to the Schrödinger equation (6) is expressed in term of ρ as

$$\psi^\sigma_{nm}(\rho) = \begin{cases} C_1 e^{-\rho^2/4}\rho^{|m|}M(-a_1, b, \rho^2/2) & \rho < \sqrt{2s} \\ C_2 e^{-\rho^2/4}\rho^{|m|}U(-a_2, b, \rho^2/2) & \rho \geq \sqrt{2s}, \end{cases} \tag{12}$$

where $a_1 = \beta_\sigma - |m|/2 - 1/2$, $a_2 = \beta_0 - |m|/2 - 1/2 = a_1 - \sigma g_{\text{eff}} m^*/4$, and $b = |m|+1$. s is the dimensionless parameter defined by $s = B\pi R^2/(h/e) = \Phi/\Phi_0$; $\Phi = B\pi R^2$ and $\Phi_0 = h/e$. It determines the magnetic flux Φ passing through the quantum dot region in the unit of the flux quantum Φ_0. At the edge of the dot where $r = R$, we have the corresponding $\rho = \sqrt{2s}$. Now, C_1 and C_2 are constants satisfying the normalization condition $\int_0^{2\pi}\int_0^\infty \Psi^*\Psi r dr d\phi = 1$. From the definition of a_1, the eigenenergy can be expressed as

$$\epsilon^\sigma_{nm} = a_1 + \frac{m}{2} + \frac{|m|}{2} + \frac{1}{2} - \frac{\sigma g_{\text{eff}} m^*}{4}. \tag{13}$$

To find the values of a_1, we match the radial wavefunctions inside and outside the quantum dot by the boundary condition, i.e., the logarithmic derivatives of the wavefunctions at the dot radius ($\rho = \sqrt{2s}$)

$$\frac{\mathrm{d}}{\mathrm{d}\rho}\ln\psi^{in}(\rho)\Big|_{\rho=\sqrt{2s}} = \frac{\mathrm{d}}{\mathrm{d}\rho}\ln\psi^{out}(\rho)\Big|_{\rho=\sqrt{2s}}. \tag{14}$$

This Eq. leads to

$$a_1 - a_1\frac{M(1-a_1, b, s)}{M(-a_1, b, s)} = a_2 + a_2(a_2+b-1)\frac{U(1-a_2, b, s)}{U(-a_2, b, s)}, \tag{15}$$

which can be solved numerically to obtain the quantized values of a_1.

When g_{eff} is extremely large, it is obvious that the giant Zeeman potential $-\sigma g_{\text{eff}} m^*/4$ in Eq. (6) will greatly lower the energy levels of spin up states $\psi^{\uparrow}_{nm}(\rho)$. Then, the states are strongly confined in a very deep quantum well which is formed by the Zeeman potential existing inside the dot region. In this circumstance, we could assume that the spin up wavefunctions only distribute inside the dot region and vanish at the dot radius. With this approximation, the wavefunctions in Eq. (12) for spin up states become

$$\psi^{\uparrow}_{nm}(\rho) = Ae^{-\rho^2/4}\rho^{|m|}M(-a_1, b, \rho^2/2), \tag{16}$$

where $\psi^{\uparrow}_{nm}(\rho = \sqrt{2s}) = 0$. This boundary condition leads to

$$M(-\beta_\sigma + \frac{|m|}{2} + \frac{1}{2}, |m| + 1, s) = 0. \tag{17}$$

Defining α^M_n as the n^{th} zero of the Kummer-M function, which satisfies $M(\alpha^M_n, |m|+1, s) = 0$, we obtain the approximated eigenenergies $(\epsilon^{\uparrow}_{app})$ corresponding to the spin up states

$$\epsilon^{\uparrow}_{app} = -\alpha^M_n + \frac{m}{2} + \frac{|m|}{2} + \frac{1}{2} - \frac{g_{\text{eff}} m^*}{4}. \tag{18}$$

Conversely, the giant Zeeman potential $-\sigma g_{\text{eff}} m^*/4$ will act as a very high barrier for spin down states, which does not allow the states to enter the dot region. In this case, we could assume that the spin down wavefunctions only distribute outside the dot region and vanish at the dot radius to get

$$\psi^{\downarrow}_{nm}(\rho) = Be^{-\rho^2/4}\rho^{|m|}U(-a_2, b, \rho^2/2), \tag{19}$$

where $\psi^{\downarrow}_{nm}(\rho = \sqrt{2s}) = 0$. This boundary condition leads to

$$U(-\beta_0 + \frac{|m|}{2} + \frac{1}{2}, |m| + 1, s) = 0. \tag{20}$$

Defining α^U_n as the n^{th} zero of the Kummer-U function, which satisfies $U(\alpha^U_n, |m|+1, s) = 0$, we obtain the approximated eigenenergies $(\epsilon^{\downarrow}_{app})$ corresponding to the spin down states

$$\epsilon^{\downarrow}_{app} = -\alpha^U_n + \frac{m}{2} + \frac{|m|}{2} + \frac{1}{2}. \tag{21}$$

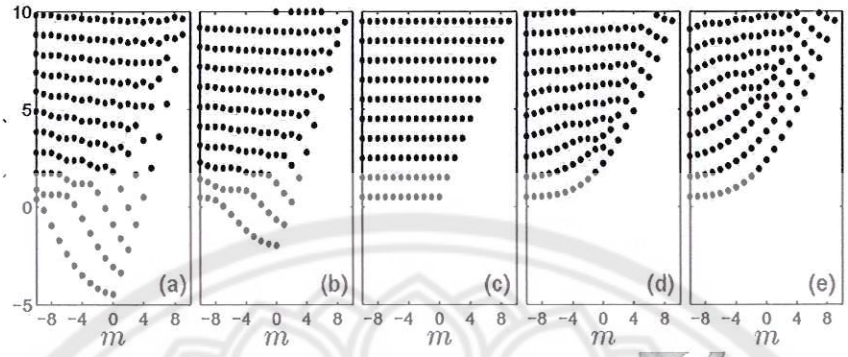

Figure 2: The energy spectrum of spin up and spin down eigenstates for various values of g_{eff}. (a) $E^{\uparrow}$ with $g_{\text{eff}} = 40$, (b) $E^{\uparrow}$ with $g_{\text{eff}} = 20$, (c) $E^{\uparrow}$ and $E^{\downarrow}$ with $g_{\text{eff}} = 0$, (d) $E^{\downarrow}$ with $g_{\text{eff}} = 20$, and (e) $E^{\downarrow}$ with $g_{\text{eff}} = 40$.

3. Results and discussion

After solving Eq. (15) numerically, we obtain the quantized values of a_1 for spin up and spin down states, leading to the spin-dependent eigenenergies in Eq. (13) as shown in Fig. 2. In this calculation, $m^* = 0.5$ and $s = 4$, corresponding to a quantum dot radius $R = 100$ nm and a magnetic field of 0.5 T. To see the effect of the giant Zeeman potential clearly, the value of g_{eff} is varied in each panel of the figure. Note that g_{eff} can be controlled by temperature, magnetic concentration, and host semiconductors in experiments.

Without the Zeeman potential ($g_{\text{eff}} = 0$), spin up and spin down states have the same energies as seen in Fig. 2(c). Because electrons only feel a uniform magnetic field, their energy levels are exactly the same as the well-known Landau levels [30]: $\epsilon = n + m/2 + |m|/2 + 1/2$. When g_{eff} is greater than zero, electrons additionally feel the discontinuous Zeeman potential. This leads to the energy spectrum which can be considered as Landau levels disturbed by the exchange interaction in a DMS region.

In Fig. 2(a) and (b), we see that some low-lying energy levels of spin up states tend to separate from the others with increasing of g_{eff}, resulting in two

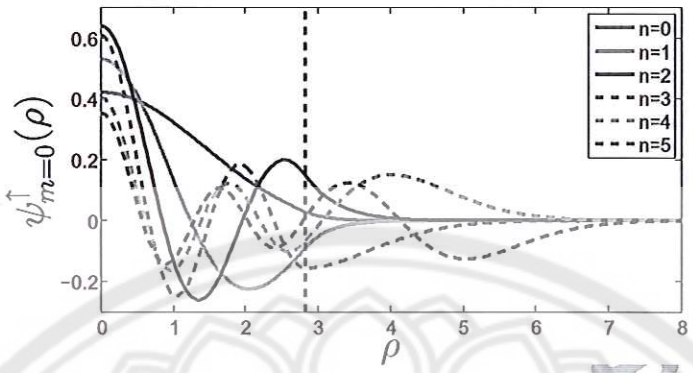

Figure 3: Spin up radial wavefunctions with $m = 0$ corresponding to the eigenenergies in Fig. 2(a) where $g_{\text{eff}} = 40$. The black dashed line represents the dot radius where $\rho = \sqrt{8}$.

energy patterns concerning the distribution of wavefunctions. Examples of low-lying states represented by solid lines are shown in Fig. 3. Their energies are negative because the negative Zeeman potential $-g_{\text{eff}}m^*/4$ in Eq. (6) behaves like a quantum well to trap the states. For this reason, they are mostly localized inside the dot region and start decaying when extending outside. The high-energy excited states represented by dashed lines behave differently. Due to their positive energies, they are not confined by the Zeeman quantum well. As seen in Fig. 3, the states oscillate over the region both inside and outside the dot.

In the case of the spin down spectrum shown in Fig. 2(d) and (e), the Zeeman potential $g_{\text{eff}}m^*/4$ existing in the DMS region will act as a barrier to perturb Landau levels by raising the energy levels. We find low-lying states are pushed by the Zeeman barrier to the region outside. As seen in Fig. 4, the states with $n = 0, 1$, and 2 oscillate outside and decay when extending inside the dot region. If energies of excited states are greater than the Zeeman potential $g_{\text{eff}}m^*/4$, they will be able to extend over the region both inside and outside the dot. As seen in the figure, the states $\psi^{\downarrow}_{n=3,4,5}$ with energies 5.606, 6.095, and 7.099 can oscillate in the DMS region, where the Zeeman potential in the figure is $g_{\text{eff}}m^*/4 = 5$. Note that all energies are in the unit of $\hbar\omega_c$. Raising the value

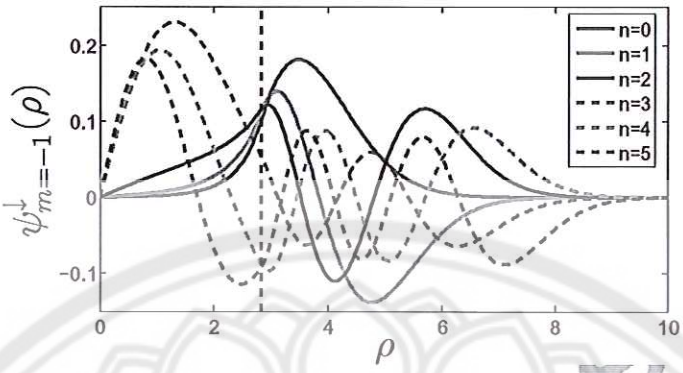

Figure 4: Spin down radial wavefunctions with $m = -1$ corresponding to the eigenenergies in Fig. 2(e) where $g_{\text{eff}} = 40$. The black dashed line represents the dot radius where $\rho = \sqrt{8}$

of g_{eff} will increase the number of the states which decay inside the dot region.

When $|m|$ is sufficiently large, both spin up and spin down states will behave like Landau states. Considering Eq. (6), one can see that the term $m^2/2\rho^2$ acts as a barrier which does not allow wavefunctions to enter the center of the quantum dot. As a result, the wavefunctions with large $|m|$ will extend far from the origin. In a classical viewpoint, electrons corresponding to the states with large $|m|$ will travel outside the dot region where the magnetic field is uniform and the Zeeman potential is zero. They do not feel the discontinuous Zeeman potential. Consequently, their eigenenergies and eigenstates are similar to Landau levels and Landau states respectively.

Fig. 5 shows the approximated eigenenergies of spin up and spin down states in the circumstance where the giant Zeeman potential is extremely large (g_{eff}=500). We find that our spin up approximation agrees well with the eigenenergies of low-lying states with small $|m|$. This is because the spatial distribution of high energy states and the states with large $|m|$ is not consistent with the assumption in our approximation; they can penetrate deep into the region outside. On the other hand, the approximated eigenenergies of spin down states are found to be in good agreement when $|m|$ is sufficiently large. For each value of m, we see that the energies of excited states tend to differ from approximated

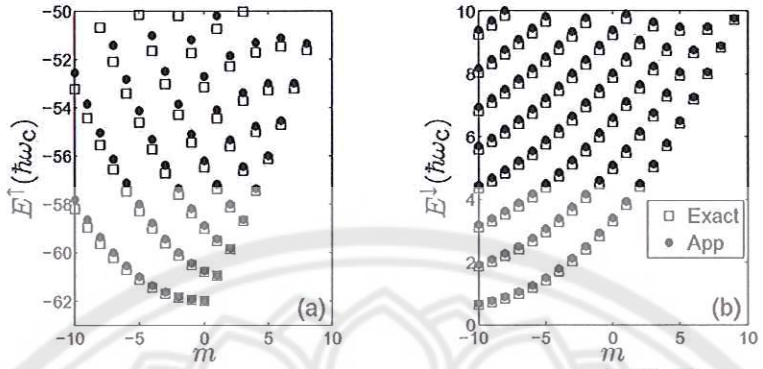

Figure 5: Comparison of exact eigenenergies (squares) and approximated energies (points) when g_{eff} is 500, $s = 6$, and $m^* = 0.5$ for (a) spin up and (b) spin down.

values. This is because these states can penetrate deep into the dot region.

In conclusion, we have presented the quantum dot heterostructure of a DMS and a NMS in the presence of a uniform magnetic field, where a band offset at a mismatched interface is vanishingly small, compared to the giant Zeeman splitting. Spin-dependent eigenenergies and eigenstates describing electrons trapped in the quantum dot are derived by matching wavefunctions at the boundary. It is found that the Zeeman potential due to the exchange interaction in a DMS can be used to control the spin distribution of low-lying states. That is, spin up states are confined inside the dot region, while spin down states extend outside. If energies of spin states are sufficiently large, they will be able to distribute over the region both inside and outside the dot. These results may be useful for manipulating spin states in spintronic application. However, for the heterostructure where a band offset is significant the spin-dependent localization will not be found. We also calculate the approximated eigenenergies when g_{eff} is very large. Good approximation is found when spin up wavefunctions are strongly localized inside the dot area and spin down wavefunctions overwhelmingly distribute outside.

4. Acknowledgements

This work was financially supported by Naresuan University Research Grants.

References

References

[1] J. K. Furdyna, Diluted magnetic semiconductors: An interface of semiconductor physics and magnetism (invited), J. Appl. Phys. 53 (1982) 7637–7643.

[2] J. K. Furdyna, Diluted magnetic semiconductors, J. Appl. Phys. 64 (1988) R29–R64.

[3] W. de Jonge, H. Swagten, Magnetic properties of diluted magnetic semiconductors, J. Magn. Magn. Mater. 100 (1991) 322–345.

[4] A. Hundt, J. Puls, F. Henneberger, Spin properties of self-organized diluted magnetic Cd_{1-x} Mn_x Se quantum dots, Phys. Rev. B 69 (2004) 121309.

[5] T. Dietl, M. Sawicki, M. Dahl, D. Heiman, E. D. Isaacs, M. J. Graf, S. I. Gubarev, D. L. Alov, Spin-flip scattering near the metal-to-insulator transition in $Cd_{0.95}$ $Mn_{0.05}$ Se:In, Phys. Rev. B 43 (1991) 3154–3163.

[6] P. Kacman, Spin interactions in diluted magnetic semiconductors and magnetic semiconductor structures, Semicond. Sci. Technol. 16 (2001) R25.

[7] I. Žutić, J. Fabian, S. Das Sarma, Spintronics: Fundamentals and applications, Rev. Mod. Phys. 76 (2004) 323–410.

[8] T. G. Rappoport, M. Berciu, B. Jankó, Effect of the Abrikosov vortex phase on spin and charge states in magnetic semiconductor-superconductor hybrids, Phys. Rev. B 74 (2006) 094502.

[9] M. Berciu, B. Jankó, Nanoscale Zeeman localization of charge carriers in diluted magnetic semiconductor-permalloy hybrids, Phys. Rev. Lett. 90 (2003) 246804.

[10] X. L. Wang, C. T. Lin, B. Liang, S. Yu, S. Ooi, K. Hirata, S. Y. Ding, D. Q. Shi, S. X. Dou, Z. W. Lin, J. G. Zhu, Josephson-vortex flow resistance in $Bi_2Sr_2Ca_2Cu_3O_y$ single crystals and its possible application in the manipulation of spin and charge textures in diluted magnetic semiconductors, J. Appl. Phys. 101 (2007) 09G116.

[11] J. C. Egues, Spin-dependent perpendicular magnetotransport through a tunable $ZnSe/Zn_{1-x}Mn_xSe$ heterostructure: A possible spin filter?, Phys. Rev. Lett. 80 (1998) 4578–4581.

[12] K. Chang, F. Peeters, Spin polarized tunneling through diluted magnetic semiconductor barriers, Solid State Commun. 120 (2001) 181 – 184.

[13] Y. Guo, H. Wang, B.-L. Gu, Y. Kawazoe, Spin-polarized transport through a $ZnSe/Zn_{1-x}Mn_xSe$ heterostructure under an applied electric field, J. Appl. Phys. 88 (2000) 6614–6617.

[14] F. Zhai, Y. Guo, B.-L. Gu, Effects of conduction band offset on spin-polarized transport through a semimagnetic semiconductor heterostructure, J. Appl. Phys. 90 (2001) 1328–1332.

[15] A. Saffarzadeh, The effects of mn concentration on spin-polarized transport through ZnSe/ZnMnSe/ZnSe heterostructures, Solid State Commun. 137 (2006) 463 – 468.

[16] W. Xu, Y. Guo, Spin-dependent transport in diluted-magnetic-semiconductor/semiconductor quantum wires, J. Appl. Phys. 100 (2006) 033901.

[17] J.-Q. Lu, Y. Guo, F. Zhai, B.-L. Gu, J.-Z. Yu, Y. Kawazoe, Spin-polarized transport through a magnetic heterostructure: tunneling and spin filtering effect, Phys. Lett. A 299 (2002) 616 – 621.

[18] X. G. Guo, J. C. Cao, A fully spin-polarized two-dimensional free electron gas induced in narrow diluted magnetic semiconductor quantum wells by in-plane magnetic fields, Semicond. Sci. Technol. 21 (2006) 341.

[19] X. J. Li, K. Chang, Electric-field tuning s-d exchange interaction in quantum dots, Appl. Phys. Lett. 92 (2008) 071116.

[20] K. Chang, S. S. Li, J. B. Xia, F. M. Peeters, Electron and hole states in diluted magnetic semiconductor quantum dots, Phys. Rev. B 69 (2004) 235203.

[21] A. J. Peter, K. L. M. Eucharista, Optically induced magnetization in diluted magnetic quantum dots, J. Magn. Magn. Mater. 321 (2009) 402 – 407.

[22] D. Lalitha, A. J. Peter, C. K. Yoo, Effects of sp-d exchange on a bound polaron and the g-factor of the exciton in a GaMnAs quantum dot, Superlattices Microstruct. 60 (2013) 453 – 461.

[23] F. V. Kyrychenko, J. Kossut, Diluted magnetic semiconductor quantum dots: An extreme sensitivity of the hole Zeeman splitting on the aspect ratio of the confining potential, Phys. Rev. B 70 (2004) 205317.

[24] T. Tomita, A. Uetake, T. Asahina, K. Kayanuma, A. Murayama, Y. Oka, Spin injection processes in ZnSe-based double quantum dots of diluted magnetic semiconductors, J. Supercond. Nov. Magn. 18 (2005) 405–410.

[25] M. Triki, S. B. Afia, S. Jaziri, Electron states in CdMnSe/ZnSe and in CdSe/ZnMnSe diluted magnetic semiconductor quantum dots, Phys. Stat. Sol. (c) 6 (2009) 845–848.

[26] N. Kim, H. Kim, T. W. Kang, Manipulation of spin states by dipole polarization switching, Appl. Phys. Lett. 91 (2007) 113504.

[27] H. Kim, N. Kim, Manipulation of spin distribution in double quantum disks with external magnetic field, Semicond. Sci. Technol. 24 (2009) 095015.

[28] L. Jiang, X. Liu, Z. Zhang, R. Wang, Manipulating the spin states in a double molecular magnets tunneling junction, Phys. Lett. A 378 (2014) 426 – 430.

[29] M. Abramowitz, I. A. Stegun, Handbook of mathematical functions with-
220 formulas, graphs, and mathematical tables, Dover Publications, New York, 1970.

[30] L. D. Landau, E. M. Lifshitz, Quantum Mechanics (Non-relativistic Theory), 3 ed., BPC Wheatons Ltd, Exeter, 1977.

Highlights.

-A DMS/NMS quantum dot is theoretically studied.

- The effective mass approximation is used.

-The effects of the giant Zeeman splitting are investigated.

-The spin-dependent distribution of spin states is found.

Superlattices and Microstructures 80 (2015) 72–79

Contents lists available at ScienceDirect

Superlattices and Microstructures

journal homepage: www.elsevier.com/locate/superlattices

A magnetic quantum dot in a diluted magnetic semiconductor/semiconductor heterostructure ☆

A. Amthong *

Department of Physics, Faculty of Science, Naresuan University, Phitsanulok 65000, Thailand
Research Center for Academic Excellence in Applied Physics, Naresuan University, Phitsanulok 65000, Thailand

ARTICLE INFO

Article history:
Received 3 November 2014
Received in revised form 29 December 2014
Accepted 31 December 2014
Available online 8 January 2015

Keywords:
Diluted magnetic semiconductors
Quantum dot
Heterostructure

ABSTRACT

A circular quantum dot consisting of a diluted magnetic semiconductor and a nonmagnetic semiconductor in the presence of a constant magnetic field is theoretically investigated. Electron eigenenergies and eigenstates are calculated using effective mass approximation. We show how the spin up and spin down eigenenergies vary with the effective g-factor. Spin-dependent distribution of electron wavefunctions is found. The approximation of the eigenenergies is also discussed.

1. Introduction

A diluted magnetic semiconductor (DMS) [1–3] is a compound semiconductor formed by doping of a nonmagnetic semiconductor (NMS) by magnetic ions. Magnetic properties in a DMS caused by the impurities have attracted much attention. In a paramagnetic DMS, an external magnetic field gives rise to not only the normal Zeeman splitting but also the strong exchange interaction between band electrons in a DMS and those associated with magnetic ions. As a result, the energy splitting is extremely enhanced. This phenomenon can be interpreted by introducing the effective g-factor (g_{eff}) which is much larger than the g-factor of band electrons. Experimental studies show the value of g_{eff} can be tuned to several hundreds, depending upon magnetic concentration, temperature, and host semiconductors [4,5].

☆ Fully documented templates are available in the elsarticle package on CTAN.

* Address: Department of Physics, Faculty of Science, Naresuan University, Phitsanulok 65000, Thailand.
E-mail address: attapona@nu.ac.th
URL: http://www.elsevier.com

http://dx.doi.org/10.1016/j.spmi.2014.12.032
0749-6036/

According to the giant Zeeman effect, a DMS has become one of the most potential materials for spintronic application which aims to manipulate spin and charge of carriers [6,7]. One example of the application is spin polarized bound states which are created in a DMS layer in the presence of non-homogeneous magnetic fields associated with permalloy disks, Abrikosov vortices, and Josephson vortices [8–10]. When g_{eff} is sufficiently large, the Zeeman energy will become a major confinement potential, while the potential due to a magnetic vector potential can be neglected. The energy spectrum of the Zeeman-bound states is therefore found to be influenced by magnetic field profiles.

Another possibility is to use a DMS as a tunnel junction. It was first investigated by Egues [11] who focused on the ZnSe/ZnMnSe/ZnSe heterostructure. Based on the concept that spin up and spin down electrons feel different potentials in the region of a DMS, a spin-polarized current can be achieved after injected electrons tunnel through a DMS. Using the different method, Chang and Peeters [12] revisited the problem to support the work of Egues. They additionally investigated the effect of the DMS thickness on spin-dependent conductivity. In the other studies of the heterostructure [13–15], the effects of the Mn concentration, conduction band offset, and applied electric field are included to improve the spin polarization. The results from related systems consisting of DMSs also show the possibility of spin-polarized tunnelling [16–18].

Moreover, DMSs are applied to quantum dots. They have been studied for different geometries: a cylinder, a sphere, and a cuboid [19–24]. Interestingly, Triki et al. [25] proposed the quantum dot heterostructure which is formed by CdMnSe (CdSe) in the shape of a truncated cone surrounded by ZnSe (ZnMnSe) and numerically studied the variation of electron energies as a function of a magnetic field. In the heterostructure, the potential due to the band offset, which is discussed intensively, plays a major role in electron confinement while the giant Zeeman potential only leads to energy splitting of spin up and spin down states.

In this work, we analytically investigate the DMS/NMS quantum dot formed by a disk-shaped DMS surrounded by a NMS as depicted in Fig. 1, focusing on the effect of the giant Zeeman potential. To see the effect clearly, we study the quantum dot where a host semiconductor of a DMS is the same material as a surrounding NMS. In this heterostructure, only the confinement due to the giant Zeeman potential exists while the band offset at the interface can be ignored. The spin-dependent energy spectrum and distribution of electron states are discussed and classified. Without the band offset, we find spin up and spin down states exhibit completely different spatial distribution. These behaviors of spin states may be useful for the application of spin-based memories or future spintronic devices [26–28].

2. Theoretical formulations

Within the mean field approximation, the potential energy of a conduction band electron travelling in a DMS subjected to a magnetic field $\vec{B} = B\hat{z}$ is given by

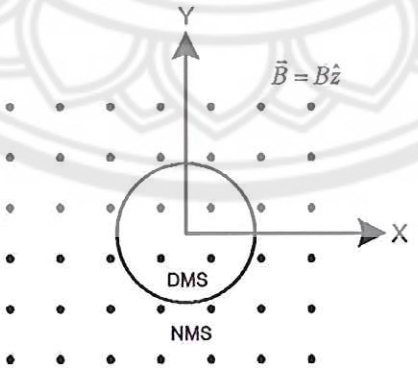

Fig. 1. The hybrid system of a circular DMS surrounded by a NMS in a uniform magnetic field $\vec{B} = B\hat{z}$ represented by the symbol •.

$$V = \frac{1}{2} g^* \mu_B \sigma_z B - \frac{1}{2} N_0 \alpha x \langle S_z \rangle \sigma_z, \tag{1}$$

where the first term is the Zeeman splitting energy and the second one is the potential associated with the exchange interaction between electrons in the conduction band and those of doped magnetic ions. In this equation, g^* is the electron g-factor, σ_z is the z component of Pauli matrices, $N_0\alpha$ is the exchange constant, x is magnetic concentration, and $\langle S_z \rangle$ is the average spin per magnetic site. Because $\langle S_z \rangle$ only exists when a magnetic field is non-vanishing. It is more convenient to write the potential as

$$V = -\frac{1}{2} g_{\text{eff}} \mu_B \sigma_z B, \tag{2}$$

where $g_{\text{eff}} = -g^* + \frac{N_0 \alpha x \langle S_z \rangle}{\mu_B B}$ is the effective g-factor [8].

In our study, the layer of DMS/NMS heterostructure placed on x–y plane in the presence of a magnetic field $\vec{B} = B\hat{z}$ is investigated. For simplicity, we assume that electrons move effectively in the plane. Within the effective mass approximation, the Hamiltonian in cylindrical coordinates (r, ϕ, z) describing a single electron $(q = -e)$ in the layer is

$$\widehat{H} = \frac{\left(\hat{p} + e\vec{A}\right)^2}{2M} - \frac{1}{2} g_{\text{eff}} \mu_B \sigma_z B \Theta(R - r), \tag{3}$$

where M is the effective mass of an electron, R is the radius of a circular DMS, and Θ is the Heaviside step function. Here, the conventional Zeeman interaction outside the dot region $(r \geqslant R)$ is vanishingly small, compared to the giant Zeeman interaction existing inside. The symmetric gauge $\vec{A} = (Br/2)\hat{\phi}$ is chosen in our calculation. Due to the rotational symmetry of the Hamiltonian, the general form of the eigenfunction can be expressed as

$$\Psi^{\sigma}_{nm}(r, \phi) = e^{im\phi} \psi^{\sigma}_{nm}(r) \chi_{\sigma}, \tag{4}$$

where n, m, and σ refer to a radial quantum number, an angular momentum and spin ($\uparrow$ or $\downarrow$) respectively. $\chi_{\uparrow\downarrow}$ is the column matrix representing a spin up $\begin{pmatrix} 1 \\ 0 \end{pmatrix}$ or spin down $\begin{pmatrix} 0 \\ 1 \end{pmatrix}$ state. After substituting the wavefunction (4) into the Schrödinger equation and using the relation $\sigma_z \chi_{\sigma} = \sigma \chi_{\sigma}$ where σ is 1 and -1 for spin up and spin down respectively, we obtain the radial equation

$$\begin{aligned} &-\frac{\hbar^2}{2M}\left(\frac{\partial^2}{\partial r^2} + \frac{1}{r}\frac{\partial}{\partial r} - \frac{m^2}{r^2}\right)\psi^{\sigma}_{nm}(r) + \left(\frac{m\hbar\omega_c}{2} + \frac{M\omega_c^2 r^2}{8}\right)\psi^{\sigma}_{nm}(r) - \left(\frac{\sigma g_{\text{eff}} \mu_B B \Theta(R - r)}{2}\right)\psi^{\sigma}_{nm}(r) \\ &= E\psi^{\sigma}_{nm}(r), \end{aligned} \tag{5}$$

where $\omega_c = eB/M$ is the cyclotron frequency. We then measure all of the quantities in the following units: $r = \rho\ell$, $E = \epsilon\hbar\omega_c$, and $M = m^* M_e$ where $\ell = \sqrt{\hbar/eB}$ is the magnetic length and M_e is the electron rest mass. The Schrödinger equation is rewritten in the dimensionless form

$$\left(-\frac{1}{2}\frac{\partial^2}{\partial \rho^2} - \frac{1}{2\rho}\frac{\partial}{\partial \rho} + \frac{m^2}{2\rho^2} + \frac{m}{2} + \frac{\rho^2}{8} - \frac{\sigma g_{\text{eff}} m^* \Theta(R/\ell - \rho)}{4}\right)\psi^{\sigma}_{nm}(\rho) = \epsilon\psi^{\sigma}_{nm}(\rho). \tag{6}$$

After that, we define another variable $x = \rho^2/2$. The Schrödinger equation now becomes

$$\left(x\frac{\partial^2}{\partial x^2} + \frac{\partial}{\partial x} - \frac{x}{4} - \frac{m^2}{4x} + \beta(x)\right)\psi^{\sigma}_{nm}(x) = 0, \tag{7}$$

where

$$\beta(x) = \begin{cases} \beta_{\sigma} & x < R^2/(2\ell^2) \\ \beta_0 & x \geqslant R^2/(2\ell^2), \end{cases} \tag{8}$$

$\beta_\sigma = \beta_0 + (\sigma g_{\text{eff}} m^*/4)$, and $\beta_0 = \epsilon - m/2$. Considering the solutions when x is close to 0 and infinity, we find the wavefunction $\psi^\sigma_{nm}(x)$ can be expressed as $\psi^\sigma_{nm}(x \to 0) = x^{|m|/2}$ and $\psi^\sigma_{nm}(x \to \infty) = e^{-x/2}$. Therefore, the general solution of Eq. (7) is given by

$$\psi^\sigma_{nm}(x) = x^{|m|/2} e^{-x/2} w(x). \tag{9}$$

To find the solution inside the quantum dot ($r < R$) where $\beta(x) = \beta_\sigma$, we substitute the wavefunction (9) into the Schrödinger Eq. (7) and yield the Kummer's equation [29]

$$x\frac{\partial^2 w}{\partial x^2} + (|m| + 1 - x)\frac{\partial w}{\partial x} - \left(\frac{|m|}{2} + \frac{1}{2} - \beta_\sigma\right) w = 0, \tag{10}$$

whose solution is

$$w(x) = C_1 M\left(\frac{|m|}{2} + \frac{1}{2} - \beta_\sigma, |m| + 1, x\right) + C_2 U\left(\frac{|m|}{2} + \frac{1}{2} - \beta_\sigma, |m| + 1, x\right), \tag{11}$$

where C_1 and C_2 are arbitrary constants. M and U are a Kummer-M function and Kummer-U function respectively. Because $x^{|m|/2} e^{-x/2} U\left(\frac{|m|}{2} + \frac{1}{2} - \beta_\sigma, |m| + 1, x\right)$ diverges when x approaches 0, we choose $C_2 = 0$ to obtain a Kummer-M function as the solution inside the quantum dot.

Outside the quantum dot region ($r \geqslant R$) where the giant Zeeman interaction vanishes, we can find the solution in the same way we did before. In this case, we also get the solution in the form of a Kummer-M function and Kummer-U function as shown in Eq. (11), but β_σ is replaced by β_0. When x approaches infinity, a Kummer-M function $M\left(\frac{|m|}{2} + \frac{1}{2} - \beta_0, |m| + 1, x\right)$ is proportional to $e^x x^{\left(-\frac{|m|}{2} - \frac{1}{2} - \beta_0\right)}$. This causes the wavefunction $\psi^\sigma_{nm}(x)$ to diverge. Hence, we choose $C_1 = 0$ in this case to get a Kummer-U function as the solution outside the quantum dot. The radial wavefunction corresponding to the Schrödinger Eq. (6) is expressed in term of ρ as

$$\psi^\sigma_{nm}(\rho) = \begin{cases} C_1 e^{-\rho^2/4} \rho^{|m|} M(-a_1, b, \rho^2/2) & \rho < \sqrt{2s} \\ C_2 e^{-\rho^2/4} \rho^{|m|} U(-a_2, b, \rho^2/2) & \rho \geqslant \sqrt{2s}, \end{cases} \tag{12}$$

where $a_1 = \beta_\sigma - |m|/2 - 1/2$, $a_2 = \beta_0 - |m|/2 - 1/2 = a_1 - \sigma g_{\text{eff}} m^*/4$, and $b = |m| + 1$. s is the dimensionless parameter defined by $s = B\pi R^2/(h/e) = \Phi/\Phi_0$; $\Phi = B\pi R^2$ and $\Phi_0 = h/e$. It determines the magnetic flux Φ passing through the quantum dot region in the unit of the flux quantum Φ_0. At the edge of the dot where $r = R$, we have the corresponding $\rho = \sqrt{2s}$. Now, C_1 and C_2 are constants satisfying the normalization condition $\int_0^{2\pi} \int_0^\infty \Psi^* \Psi r dr d\phi = 1$. From the definition of a_1, the eigenenergy can be expressed as

$$\epsilon^\sigma_{nm} = a_1 + \frac{m}{2} + \frac{|m|}{2} + \frac{1}{2} - \frac{\sigma g_{\text{eff}} m^*}{4}. \tag{13}$$

To find the values of a_1, we match the radial wavefunctions inside and outside the quantum dot by the boundary condition, i.e., the logarithmic derivatives of the wavefunctions at the dot radius ($\rho = \sqrt{2s}$)

$$\frac{\mathrm{d}}{\mathrm{d}\rho} \ln \psi^{in}(\rho)\Big|_{\rho=\sqrt{2s}} = \frac{\mathrm{d}}{\mathrm{d}\rho} \ln \psi^{out}(\rho)\Big|_{\rho=\sqrt{2s}}. \tag{14}$$

This equation leads to

$$a_1 - a_1 \frac{M(1 - a_1, b, s)}{M(-a_1, b, s)} = a_2 + a_2(a_2 + b - 1)\frac{U(1 - a_2, b, s)}{U(-a_2, b, s)}, \tag{15}$$

which can be solved numerically to obtain the quantized values of a_1.

When g_{eff} is extremely large, it is obvious that the giant Zeeman potential $-\sigma g_{\text{eff}} m^*/4$ in Eq. (6) will greatly lower the energy levels of spin up states $\psi^\uparrow_{nm}(\rho)$. Then, the states are strongly confined in a very deep quantum well which is formed by the Zeeman potential existing inside the dot region. In this circumstance, we could assume that the spin up wavefunctions only distribute inside the dot

region and vanish at the dot radius. With this approximation, the wavefunctions in Eq. (12) for spin up states become

$$\psi^{\uparrow}_{nm}(\rho) = Ae^{-\rho^2/4}\rho^{|m|}M(-a_1, b, \rho^2/2), \tag{16}$$

where $\psi^{\uparrow}_{nm}(\rho = \sqrt{2s}) = 0$. This boundary condition leads to

$$M\left(-\beta_\sigma + \frac{|m|}{2} + \frac{1}{2}, |m| + 1, s\right) = 0. \tag{17}$$

Defining α^M_n as the n^{th} zero of the Kummer-M function, which satisfies $M(\alpha^M_n, |m| + 1, s) = 0$, we obtain the approximated eigenenergies ($\epsilon^{\uparrow}_{app}$) corresponding to the spin up states

$$\epsilon^{\uparrow}_{app} = -\alpha^M_n + \frac{m}{2} + \frac{|m|}{2} + \frac{1}{2} - \frac{g_{\text{eff}}m^*}{4}. \tag{18}$$

Conversely, the giant Zeeman potential $-\sigma g_{\text{eff}}m^*/4$ will act as a very high barrier for spin down states, which does not allow the states to enter the dot region. In this case, we could assume that the spin down wavefunctions only distribute outside the dot region and vanish at the dot radius to get

$$\psi^{\downarrow}_{nm}(\rho) = Be^{-\rho^2/4}\rho^{|m|}U(-a_2, b, \rho^2/2), \tag{19}$$

where $\psi^{\downarrow}_{nm}(\rho = \sqrt{2s}) = 0$. This boundary condition leads to

$$U\left(-\beta_0 + \frac{|m|}{2} + \frac{1}{2}, |m| + 1, s\right) = 0. \tag{20}$$

Defining α^U_n as the n^{th} zero of the Kummer-U function, which satisfies $U(\alpha^U_n, |m| + 1, s) = 0$, we obtain the approximated eigenenergies ($\epsilon^{\downarrow}_{app}$) corresponding to the spin down states

$$\epsilon^{\downarrow}_{app} = -\alpha^U_n + \frac{m}{2} + \frac{|m|}{2} + \frac{1}{2}. \tag{21}$$

3. Results and discussion

After solving Eq. (15) numerically, we obtain the quantized values of a_1 for spin up and spin down states, leading to the spin-dependent eigenenergies in Eq. (13) as shown in Fig. 2. In this calculation, $m^* = 0.5$ and $s = 4$, corresponding to a quantum dot radius $R = 100$ nm and a magnetic field of 0.5 T. To see the effect of the giant Zeeman potential clearly, the value of g_{eff} is varied in each panel of the figure. Note that g_{eff} can be controlled by temperature, magnetic concentration, and host semiconductors in experiments.

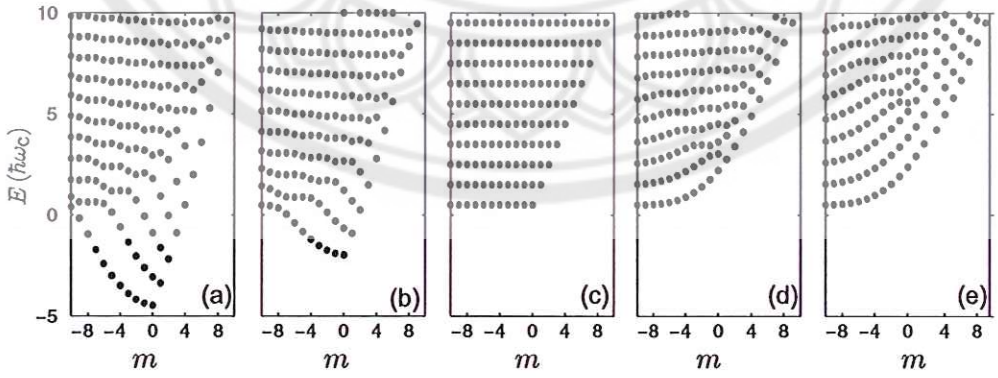

Fig. 2. The energy spectrum of spin up and spin down eigenstates for various values of g_{eff}. (a) $E^{\uparrow}$ with $g_{\text{eff}} = 40$, (b) $E^{\uparrow}$ with $g_{\text{eff}} = 20$, (c) $E^{\uparrow}$ and $E^{\downarrow}$ with $g_{\text{eff}} = 0$, (d) $E^{\downarrow}$ with $g_{\text{eff}} = 20$, and (e) $E^{\downarrow}$ with $g_{\text{eff}} = 40$.

Without the Zeeman potential ($g_{\text{eff}} = 0$), spin up and spin down states have the same energies as seen in Fig. 2(c). Because electrons only feel a uniform magnetic field, their energy levels are exactly the same as the well-known Landau levels [30]: $\epsilon = n + m/2 + |m|/2 + 1/2$. When g_{eff} is greater than zero, electrons additionally feel the discontinuous Zeeman potential. This leads to the energy spectrum which can be considered as Landau levels disturbed by the exchange interaction in a DMS region.

In Fig. 2(a) and (b), we see that some low-lying energy levels of spin up states tend to separate from the others with increasing of g_{eff}, resulting in two energy patterns concerning the distribution of wavefunctions. Examples of low-lying states represented by solid lines are shown in Fig. 3. Their energies are negative because the negative Zeeman potential $-g_{\text{eff}}m^*/4$ in Eq. (6) behaves like a quantum well to trap the states. For this reason, they are mostly localized inside the dot region and start decaying when extending outside. The high-energy excited states represented by dashed lines behave differently. Due to their positive energies, they are not confined by the Zeeman quantum well. As seen in Fig. 3, the states oscillate over the region both inside and outside the dot.

In the case of the spin down spectrum shown in Fig. 2(d) and (e), the Zeeman potential $g_{\text{eff}}m^*/4$ existing in the DMS region will act as a barrier to perturb Landau levels by raising the energy levels. We find low-lying states are pushed by the Zeeman barrier to the region outside. As seen in Fig. 4, the states with $n = 0$, 1, and 2 oscillate outside and decay when extending inside the dot region. If energies of excited states are greater than the Zeeman potential $g_{\text{eff}}m^*/4$, they will be able to extend over the region both inside and outside the dot. As seen in the figure, the states $\psi^{\downarrow}_{n=3,4,5}$ with energies 5.606, 6.095, and 7.099 can oscillate in the DMS region, where the Zeeman potential in the figure is $g_{\text{eff}}m^*/4 = 5$. Note that all energies are in the unit of $\hbar\omega_c$. Raising the value of g_{eff} will increase the number of the states which decay inside the dot region.

When $|m|$ is sufficiently large, both spin up and spin down states will behave like Landau states. Considering Eq. (6), one can see that the term $m^2/2\rho^2$ acts as a barrier which does not allow wavefunctions to enter the center of the quantum dot. As a result, the wavefunctions with large $|m|$ will extend far from the origin. In a classical viewpoint, electrons corresponding to the states with large $|m|$ will travel outside the dot region where the magnetic field is uniform and the Zeeman potential is zero. They do not feel the discontinuous Zeeman potential. Consequently, their eigenenergies and eigenstates are similar to Landau levels and Landau states respectively.

Fig. 5 shows the approximated eigenenergies of spin up and spin down states in the circumstance where the giant Zeeman potential is extremely large ($g_{\text{eff}} = 500$). We find that our spin up approximation agrees well with the eigenenergies of low-lying states with small $|m|$. This is because the spatial distribution of high energy states and the states with large $|m|$ is not consistent with the assumption in our approximation; they can penetrate deep into the region outside. On the other hand, the approximated eigenenergies of spin down states are found to be in good agreement when $|m|$ is sufficiently large. For each value of m, we see that the energies of excited states tend to differ from approximated values. This is because these states can penetrate deep into the dot region.

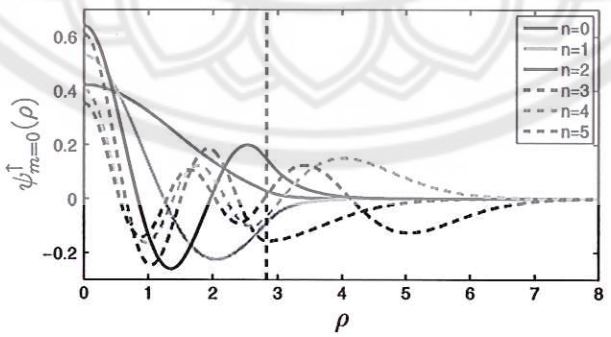

Fig. 3. Spin up radial wavefunctions with $m = 0$ corresponding to the eigenenergies in Fig. 2(a) where $g_{\text{eff}} = 40$. The black dashed line represents the dot radius where $\rho = \sqrt{8}$.

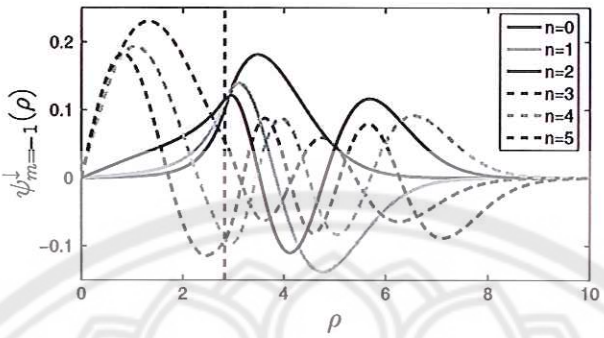

Fig. 4. Spin down radial wavefunctions with $m = -1$ corresponding to the eigenenergies in Fig. 2(e) where $g_{\text{eff}} = 40$. The black dashed line represents the dot radius where $\rho = \sqrt{8}$.

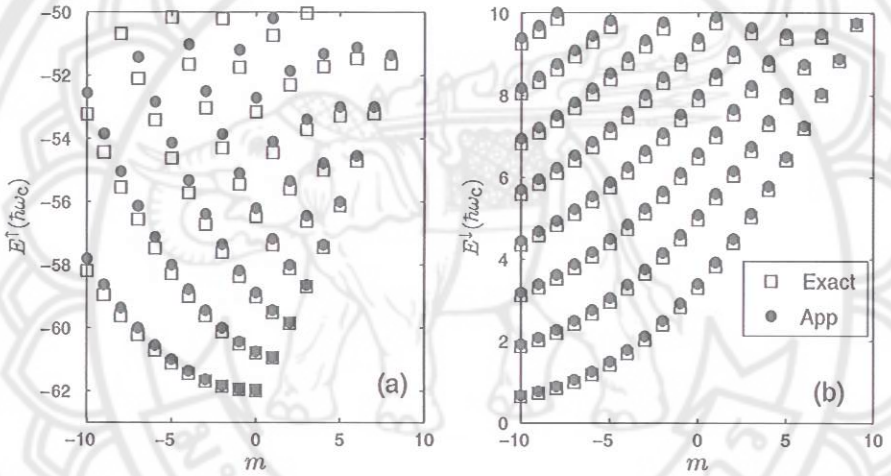

Fig. 5. Comparison of exact eigenenergies (squares) and approximated energies (points) when g_{eff} is 500, $s = 6$, and $m^* = 0.5$ for (a) spin up and (b) spin down.

In conclusion, we have presented the quantum dot heterostructure of a DMS and a NMS in the presence of a uniform magnetic field, where a band offset at a mismatched interface is vanishingly small, compared to the giant Zeeman splitting. Spin-dependent eigenenergies and eigenstates describing electrons trapped in the quantum dot are derived by matching wavefunctions at the boundary. It is found that the Zeeman potential due to the exchange interaction in a DMS can be used to control the spin distribution of low-lying states. That is, spin up states are confined inside the dot region, while spin down states extend outside. If energies of spin states are sufficiently large, they will be able to distribute over the region both inside and outside the dot. These results may be useful for manipulating spin states in spintronic application. However, for the heterostructure where a band offset is significant the spin-dependent localization will not be found. We also calculate the approximated eigenenergies when g_{eff} is very large. Good approximation is found when spin up wavefunctions are strongly localized inside the dot area and spin down wavefunctions overwhelmingly distribute outside.

Acknowledgement

This work was financially supported by Naresuan University Research Grants.

References

[1] J.K. Furdyna, Diluted magnetic semiconductors: an interface of semiconductor physics and magnetism (invited), J. Appl. Phys. 53 (1982) 7637–7643.
[2] J.K. Furdyna, Diluted magnetic semiconductors, J. Appl. Phys. 64 (1988) R29–R64.
[3] W. de Jonge, H. Swagten, Magnetic properties of diluted magnetic semiconductors, J. Magn. Magn. Mater. 100 (1991) 322–345.
[4] A. Hundt, J. Puls, F. Henneberger, Spin properties of self-organized diluted magnetic $Cd_{1-x}Mn_x$ Se quantum dots, Phys. Rev. B 69 (2004) 121309.
[5] T. Dietl, M. Sawicki, M. Dahl, D. Heiman, E.D. Isaacs, M.J. Graf, S.I. Gubarev, D.L. Alov, Spin-flip scattering near the metal-to-insulator transition in $Cd_{0.95}Mn_{0.05}$ Se:In, Phys. Rev. B 43 (1991) 3154–3163.
[6] P. Kacman, Spin interactions in diluted magnetic semiconductors and magnetic semiconductor structures, Semicond. Sci. Technol. 16 (2001) R25.
[7] I. uti, J. Fabian, S. Das Sarma, Spintronics: fundamentals and applications, Rev. Mod. Phys. 76 (2004) 323–410.
[8] T.G. Rappoport, M. Berciu, B. Jankó, Effect of the Abrikosov vortex phase on spin and charge states in magnetic semiconductor–superconductor hybrids, Phys. Rev. B 74 (2006) 094502.
[9] M. Berciu, B. Jankó, Nanoscale Zeeman localization of charge carriers in diluted magnetic semiconductor–permalloy hybrids, Phys. Rev. Lett. 90 (2003) 246804.
[10] X.L. Wang, C.T. Lin, B. Liang, S. Yu, S. Ooi, K. Hirata, S.Y. Ding, D.Q. Shi, S.X. Dou, Z.W. Lin, J.G. Zhu, Josephson-vortex flow resistance in $Bi_2Sr_2Ca_2Cu_3O_y$ single crystals and its possible application in the manipulation of spin and charge textures in diluted magnetic semiconductors, J. Appl. Phys. 101 (2007) 09G116.
[11] J.C. Egues, Spin-dependent perpendicular magnetotransport through a tunable $ZnSe/Zn_{1-x}Mn_xSe$ heterostructure: a possible spin filter?, Phys Rev. Lett. 80 (1998) 4578–4581.
[12] K. Chang, F. Peeters, Spin polarized tunneling through diluted magnetic semiconductor barriers, Solid State Commun. 120 (2001) 181–184.
[13] Y. Guo, H. Wang, B.-L. Gu, Y. Kawazoe, Spin-polarized transport through a $ZnSe/Zn_{1-x}Mn_xSe$ heterostructure under an applied electric field, J. Appl. Phys. 88 (2000) 6614–6617.
[14] F. Zhai, Y. Guo, B.-L. Gu, Effects of conduction band offset on spin-polarized transport through a semimagnetic semiconductor heterostructure, J. Appl. Phys. 90 (2001) 1328–1332.
[15] A. Saffarzadeh, The effects of mn concentration on spin-polarized transport through ZnSe/ZnMnSe/ZnSe heterostructures, Solid State Commun. 137 (2006) 463–468.
[16] W. Xu, Y. Guo, Spin-dependent transport in diluted-magnetic-semiconductor/semiconductor quantum wires, J. Appl. Phys. 100 (2006) 033901.
[17] J.-Q. Lu, Y. Guo, F. Zhai, B.-L. Gu, J.-Z. Yu, Y. Kawazoe, Spin-polarized transport through a magnetic heterostructure: tunneling and spin filtering effect, Phys. Lett. A 299 (2002) 616–621.
[18] X.G. Guo, J.C. Cao, A fully spin-polarized two-dimensional free electron gas induced in narrow diluted magnetic semiconductor quantum wells by in-plane magnetic fields, Semicond. Sci. Technol. 21 (2006) 341.
[19] X.J. Li, K. Chang, Electric-field tuning s-d exchange interaction in quantum dots, Appl. Phys. Lett. 92 (2008) 071116.
[20] K. Chang, S.S. Li, J.B. Xia, F.M. Peeters, Electron and hole states in diluted magnetic semiconductor quantum dots, Phys. Rev. B 69 (2004) 235203.
[21] A.J. Peter, K.L.M. Eucharista, Optically induced magnetization in diluted magnetic quantum dots, J. Magn. Magn. Mater. 321 (2009) 402–407.
[22] D. Lalitha, A.J. Peter, C.K. Yoo, Effects of sp-d exchange on a bound polaron and the g-factor of the exciton in a GaMnAs quantum dot, Superlattices Microstruct. 60 (2013) 453–461.
[23] F.V. Kyrychenko, J. Kossut, Diluted magnetic semiconductor quantum dots: an extreme sensitivity of the hole Zeeman splitting on the aspect ratio of the confining potential, Phys. Rev. B 70 (2004) 205317.
[24] T. Tomita, A. Uetake, T. Asahina, K. Kayanuma, A. Murayama, Y. Oka, Spin injection processes in ZnSe-based double quantum dots of diluted magnetic semiconductors, J. Supercond. Nov. Magn. 18 (2005) 405–410.
[25] M. Triki, S.B. Afia, S. Jaziri, Electron states in CdMnSe/ZnSe and in CdSe/ZnMnSe diluted magnetic semiconductor quantum dots, Phys. Stat. Sol. (c) 6 (2009) 845–848.
[26] N. Kim, H. Kim, T.W. Kang, Manipulation of spin states by dipole polarization switching, Appl. Phys. Lett. 91 (2007) 113504.
[27] H. Kim, N. Kim, Manipulation of spin distribution in double quantum disks with external magnetic field, Semicond. Sci. Technol. 24 (2009) 095015.
[28] L. Jiang, X. Liu, Z. Zhang, R. Wang, Manipulating the spin states in a double molecular magnets tunneling junction, Phys. Lett. A 378 (2014) 426–430.
[29] M. Abramowitz, I.A. Stegun, Handbook of Mathematical Functions with Formulas, Graphs, and Mathematical Tables, Dover Publications, New York, 1970.
[30] L.D. Landau, E.M. Lifshitz, Quantum Mechanics (Non-relativistic Theory), third ed., BPC Wheatons Ltd., Exeter, 1977.